ARCHIVES OF TRANSPORT *ISSN (print): 0866-9546*
Volume 72, Issue 4, 2024 ***e-ISSN (online):*** *2300-8830*
DOI: *10.61089/aot2024.eb2hfe27*

IMPACT OF WIEDEMANN 74 AND WIEDEMANN 99 CAR-FOLLOWING MODELS ON ESTIMATING LEVEL OF SAFETY AND EMISSIONS ON SIGNAL-CONTROLLED INTERSECTIONS USING MICROSCOPIC SIMULATIONS

Konrad BISZKO[1], Jacek OSKARBSKI[2], Karol ŻARSKI[3]

[1,2,3] Gdańsk University of Technology, Faculty of Civil and Environmental Engineering, Department of Transportation Engineering, Gdańsk, Poland

Abstract:

This paper examines the influence of two selected car-following models on the outcomes of microscopic traffic simulations. The authors begin by reviewing the literature on the various traffic models, methods for estimating energy consumption, fuel use, and emissions. The authors discuss using surrogate safety measures derived from analysing vehicle trajectories in a microscopic traffic model to estimate safety levels. This paper also outlines the authors' approach to data acquisition and processing at the chosen test site. Most data are sourced from the city's Intelligent Transport System (ITS) services, including traffic flow volume, vehicle speed, and public transport travel times. The data gathered from Automatic Vehicle Location (AVL) systems was compared to manual travel time measurements. Depending on the analysed section Mean Average Error (MAE) ranging from 3 to 5 seconds was obtained, however, Mean Absolute Percentage Error (MAPE) ranged from 7.46% to 30.01%. The proposed method aims to evaluate the precision of the microscopic model in replicating real road networks and traffic based on available datasets. Two car-following models (CFM), Wiedemann 74 (W74), and Wiedemann 99 (W99) are chosen for further analysis. The models were validated using the GEH statistic and by comparing speed distributions. Both the models yielded satisfactory results. Different scenarios involving changes in traffic flow and to traffic signal configurations were analysed. While both W74 and W99 yielded satisfactory results, there were discernible disparities in the analyses. In general, W99 yields less favourable results, characterised by emissions, and delays compared to W74. Depending on the scenarios compared, the number of conflicts for W74 varied up to 56% (scenarios 2 and 4), and up to 78% for W99 (scenarios 1 and 4). The methodology presented by the authors can be used in future research to analyse various traffic control solutions concerning their impact on the environment and traffic safety. The observed differences underscore the importance of careful model selection and presented approach can serve as a foundation for developing guidelines for microscopic modelling and a multi-criteria approach to selecting the most effective implementation scenarios.

Keywords: *traffic modelling, car-following models, modelling safety, modelling emissions, microscopic traffic simulations*

To cite this article:

Biszko, K., Oskarbski, J., Żarski, K., (2024). Impact of Wiedemann 74 and Wiedemann 99 car-following models on estimating level of safety and emissions on signal-controlled intersections using microscopic simulations. Archives of Transport, 72(4), 43-73. https://doi.org/10.61089/aot2024.eb2hfe27

Contact:
1) konrad.biszko@pg.edu.pl [https://orcid.org/0000-0002-6877-7348] – corresponding author; 2) jacek.oskarbski@pg.edu.pl [https://orcid.org/0000-0003-0651-4902]; 3) karol.zarski@pg.edu.pl [https://orcid.org/0000-0003-2848-0790]

1. Introduction

Global energy demand increases every year (Ritchie et al., 2024). Up to 84.3% of the energy needed for transportation, heating, and electricity production comes from fossil fuels, while the remaining 15.7% is obtained from low-carbon sources. Taking into account only electricity production, 63.3% comes from fossil fuels. The above values result in the emission of harmful substances into the environment, which affects people's health and quality of life. The unsustainable growth of transportation activities puts a strain on the ecosystems and resources of the planet. Greenhouse gas (GHG) emissions from energy production are one of the main causes of climate change. In Europe, GHG emissions were subject to a decrease between 1990 and 2017, except for the transportation sector (EEA, 2024). The transport sector is responsible for 20% of total GHG and 30% of total energy consumption in the European Union. Road transport accounts for the largest share of GHG, at 72%. (Ajanovic & Haas, 2017; EEA, 2024). Over the past few years, new and increasingly stringent emission standards have emerged, resulting in declining emissions from newly manufactured cars. However, a comparable share of carbon dioxide production by road transport has been maintained for years (Roselló et al., 2016).

Due to the observed slow transition to alternative fuel sources and energy-efficient propulsion, the transport sector is blamed for the possible non-fulfilment by individual countries of their commitments under international climate change agreements (Sims et al., 2014). For this reason, transport continues to be at the centre of any debate on energy conservation due to its dependence on fossil fuels for both passenger and freight transport. (Oskarbski & Biszko, 2023). There are many indications that the electrification of transport may not be fast enough to achieve energy-efficient and low-carbon targets for the road transport sector. (Creutzig et al., 2018; Masson-Delmotte et al., 2018). Because of the above, efforts should be made to compensate for the growth in energy demand as much as possible. The trends observed in transport development call for measures to reduce energy consumption increase decarbonisation, and improve road safety.

Assessing the effectiveness of such measures is possible using transport models that estimate energy consumption and emissions and allow the level of change in road safety to be analysed. In the context of the transportation sector, especially road transport, three main components can be identified: people, vehicles, and infrastructure. All of these elements will have an impact on the evolution of traffic energy demand as well as on road traffic safety.

The United Nations (UN) indicated that improving public health is a fundamental goal of sustainable global development (United Nations, 2015). Road traffic injuries are currently a major public health issue in society and their cause can be blamed on malfunctioning road transport systems. The problem is global and occurs in both industrialised and developing countries.

International comparisons on road safety can be made using the demographic road fatality rate (RFR), among others (Jamroz et al., 2019). Taking the RFR into account, a country's level of road safety varies non-linearly and follows its socioeconomic development as measured by Gross Domestic Product per capita (Jamroz et al., 2019; Law et al., 2011). Developing countries are in the upward phase of the RFR (before the turning point) and industrialised countries are in the downward phase (after the turning point) (Jamroz et al., 2019). It is crucial for developing countries to work towards reversing the deteriorating trend of road safety levels. Despite the downward trend in RFR in developing countries, it is imperative to sustain the decline in fatalities and potentially expedite the pace of reduction. A variety of factors influence the degree of road safety. Globally, it is mainly determined by a country's level of socioeconomic development and the mobility of its population (Law et al., 2011; Small et al., 2023). However, traffic management solutions, such as traffic organisation and control, also impact road safety levels. Hence, it is imperative to consider this aspect in the planning and designing of traffic improvements. The decision-making process to select the best solutions in terms of changes to infrastructure and traffic management elements to improve traffic conditions and safety and reduce negative impacts on the environment and surroundings can be supported by tools such as transport models.

The main aim of this paper is to present methods and models for estimating anticipated energy demand, calculating harmful environmental emissions, and estimating traffic conflicts as surrogate measures of road traffic safety. The approach presented in this paper aims to provide a general evaluation of traffic organisation and control solutions using

a microscopic model. It represents a step towards developing a multi-criteria method for evaluating the effectiveness of changes planned or implemented in the transport system. When discussing energy, the focus is on calculating the resistance to movement that a vehicle experiences. The engine must produce a specific amount of energy to overcome this resistance. This value allows for estimating the electrical energy consumption of electric vehicles (EVs). Since fuel is used to generate energy in internal combustion engines (ICE), similar approach enables estimating fuel consumption for ICE vehicles. The approach outlined in this paper allows the results to be utilised for estimating pollutant emissions, specifically focusing on carbon dioxide emissions. The results for greenhouse gas emissions and other emissions can be used, among other things, to assess the impact of traffic control strategies on energy efficiency, the environment, traffic efficiency and safety.

Section 2 provides an overview of traffic modelling issues, focusing on the methods used in microscopic-level modelling for simulating motor vehicle traffic, estimating harmful emissions from motor vehicle traffic, the number of traffic conflicts representing the level of road traffic safety and the validation processes of microscopic models. Section 3 describes the methodology for the study, including modelling the transport network in the simulation area, modelling driver behaviour, analysing public transport vehicle travel time (TT) data, and estimating emissions and traffic safety surrogate measures. Section 4 explains the process of calibrating and validating model elements, including traffic volumes, speed distributions, and travel times. The calibrated and validated models were used to conduct comparative research. The results of the study are presented in Section 5. The research results obtained using selected CFMs in the traffic simulation models were carried out according to the methodology described. The research considers examples of traffic control scenarios and different levels of traffic volumes. The results enable a comparative analysis of the application of the selected CFMs in terms of vehicle delays, energy and emissions consumption, and the number and type of traffic conflicts. Section 6 discusses the issues presented. Section 7 contains the conclusions of the research presented in the paper. The wide range of results presented in the article is a prelude to developing a multi-criteria evaluation of the improvements implemented at intersections. Such an assessment can be extremely helpful in selecting the best solutions for the required traffic organisation and traffic control improvements.

2. Literature review

The European Commission (Wefering et al., 2014) recommends using different methods and tools to increase the efficiency of the planning and decision-making processes. Transport models are used for planning, decision-making, and monitoring processes of implemented measures. Transport models can provide much-needed support for planning and decision-making (Givoni et al., 2016) and supplement engineering knowledge and practice with the results of simulations conducted in the model. The results generated by the transport model can provide essential information on existing or future transport problems that arise from changing mobility patterns, urban spatial development, and planned or ongoing transport projects. With a range of applications that can serve different municipal or road authorities, it can support a range of activities, from planning the transport system to local traffic management at the operational level. Developing a new model or updating it requires funding and qualified staff. The cost of building a model depends on its complexity and the size of the city or area requiring modelling, which can sometimes be a real barrier. Human and financial resources are needed to maintain and improve the model. Many towns and rural road administrations do not have a transport model, probably due to the anticipated costs of building and maintaining one. Transport models require money, personnel staff, and time, and decision-makers do not always appreciate the benefits. As a result, the decision to work with a model should only be made if the costs and benefits are properly understood. Transport models allow for the representation of the flow of people and goods in a transport network in an area with specific socioeconomic and land use characteristics (Sivakumar, 2007). These tools help simulate the behaviour of the city's transport system and its users, with the system's response to transport supply and demand changes. In the second half of the twentieth century, there was extensive research on mathematical modelling of transport networks, travel demand, and vehicle flows (Singh & Dowling, 1999). As a result of this research, many software packages have been developed to help develop models of

transport systems for a given area and elements of the road network, taking traffic and travel forecasting into account (Barcelo, 2010).

There are different approaches to traffic modelling, depending on the transport system elements studied, the study's area scope, and the expected results. Transport demand and street network models can be developed at varying levels of detail: macroscopic, mesoscopic, or microscopic (Gerlough & Huber, 1975). The most commonly used models for planning purposes are macroscopic models (e.g., the integrated transport and land use model or the four-stage travel demand model) (Gavanas et al., 2016; Wefering et al., 2014). For strategic studies, macroscopic models are commonly used in developing land use and transport plans or planning large-scale road networks and public transport routes. Macroscopic models are generally designed to research the movement of people, goods, or vehicles across a broad area with a lower level of detail, primarily due to limitations in survey tools and data availability (Alonso et al., 2017; Oskarbski et al., 2021). Planning software that uses macroscopic models facilitates the analysis of changes in transport demand resulting from variations in land use, socioeconomic factors, and demographic data. It also allows for the analysis of modal split and modal shift between different transport modes resulting from changes in the transport system. For modelling purposes, a macroscopic approach, like a four-stage model, is employed (Bonnafous et al., 2013; Ortuzar et al., 2011). This approach comprises two fundamental components: transport network and travel demand models. These models consider deterministic characteristics of a traffic stream, such as speed, flow, and density. The resulting values are usually aggregated, e.g. the average number of vehicles per day or peak hour. The modelling results can provide a platform for estimating delays, emissions and safety for a specific and extensive road network (Ambroziak et al., 2015; Gore et al., 2023; Jacyna et al., 2017, 2021, 2022). The disadvantage of this approach is the relative lack of precision. Some aspects present in the road network, such as local conditions, individual driver behaviour and specific traffic management measures, may not be possible to take into account when implementing a large-scale model.

In cases where more detail is required, mesoscopic and microscopic models are essential, as they help to simulate traffic flows with their profiles, platoon dispersion, averaged traffic parameters such as queues and delays, saturation flows, etc. (mesoscopic models) and the behaviour of traffic participants and interactions between individual road users (microscopic models). Mesoscopic models combine macroscopic and microscopic approaches but provide less reliable information than microscopic models. Mesoscopic models make it possible to simulate and study the movement of vehicle groups in road sections and intersections (Jayakrisham et al., 1994). Mesoscopic models enable the identification of critical elements in the transport network regarding traffic conditions (due to queues and delays). They also help to analyse ways to improve traffic efficiency, such as changes in traffic organisation, adjustments to traffic signal programmes, and modifications to the geometry of road network elements. These measures can improve transport efficiency and road safety (Kristoffersson, 2013; Sider et al., 2014). The analyses cover the impact of planned improvements on the entire transport network of a city or region, road sections with multiple intersections or individual intersections.

A microscopic approach can be used for an accurate analysis. Microscopic models enable the modelling of complex urban street network systems, multimodal systems, pedestrian traffic, traffic signals, and interchanges. In this approach, each vehicle and pedestrian is represented as a separate object (May, 1990). Due to the higher level of detail, it is possible to simulate the interaction between the individual objects (Szarata et al., 2023). Consequently, there are higher computational requirements for the modelling. Furthermore, to properly develop the microscopic analysis, more time is needed to model the individual road network elements and calibrate the behaviour of the traffic participants. For this reason, it is not practical to consider such a large area scale as in software packages for macroscopic or mesoscopic modelling. On the other hand, the results obtained from a microscopic model are more precise. Measures such as speed and delay are obtained for each vehicle separately. Emissions can be calculated by considering vehicle dynamics and different weight distributions between light and heavy vehicles (Acuto et al., 2022; Smit et al., 2007). Models can be used for the prediction of car crash frequency (L. Wang et al., 2018). Another approach is to estimate the number of traffic conflicts by calibrating a microscopic simulation to reproduce

pedestrian-vehicle interactions based on traffic at intersections (M. S. Hussain et al., 2024). Road traffic safety can be analysed by assessing the interactions between vehicle trajectories on the road network (Cafiso et al., 2018; Hayward, 1972; Oskarbski et al., 2020; Tak et al., 2018). Microscopic models help to assess the application of different traffic control strategies, e.g., how allowing a right turn on red (RTOR) manoeuvre affects traffic conditions (Liu et al., 2024). The researchers also used a multidisciplinary approach in which they first modelled the simulated behaviour of water following heavy rainfall in the city, and then used microscopic simulation to assess how the predicted presence of water on particular road sections would affect time loss for vehicles (E. Hussain et al., 2018).

Even if the final results are presented as a sum or average value for analysis, they are often considered more precise than those derived from macroscopic or mesoscopic models because the process leading to them is more sophisticated. Microscopic traffic simulation software enables the recording of the behaviour of all individual traffic participants for each time step of the simulation based on rules set by three groups of algorithms: car-following, lane changing, and gap acceptance (Ahmed et al., 2021). Planners and researchers use various software packages for traffic studies. Various microscopic models (as discussed regarding CFM in Section 2.1) have been developed over the years and are implemented in software offered by different companies. Researchers using specialised software sometimes omit important details when selecting and calibrating models using default algorithm values. Moreover, various models and algorithms can yield different research results (Rakha & Gao, 2010). The research presented in this article, which utilised the PTV VISSIM traffic simulation software package, considered the application of two selected psychophysical car-following models.

2.1. Microscopic modelling of traffic

Theory-based CMF describes vehicle interactions using mathematical equations to represent driver behaviour. In free-flow traffic conditions, the driver can move at the desired speed. In forced traffic conditions, if the vehicle following the lead vehicle is in relative proximity, the leader's behaviour affects the car's behaviour following it. Each vehicle strives to travel at the highest possible safe speed and maintain a safe distance from the preceding vehicle. These conditions are achieved by dynamically adjusting speed (accelerating and decelerating). In the scientific literature, we can find many examples of CFM based on theory or supervised, unsupervised, and reinforcement learning (Ahmed et al., 2021; Han et al., 2022; Zhang et al., 2024). Among the theory-based models, there are kinematic models represented by the Gipps Model (Gipps, 1981; Shah et al., 2023), Newell's Model (Meng et al., 2021; Newell, 2002), Cellular Automata models (CA) (Benjamin et al., 1996), General Motors models (GM) also known as GHR (Gazis-Herman-Rothery) model (Gazis et al., 1961), Optimal Velocity Model (OVM) (Shang et al., 2022; Si et al., 2023) and Intelligent Driver Model (IDM) (Zhou et al., 2024). The second group of theory-based models is psychophysical models, of which we can mention the Action Point Model (APM) (W. H. Wang et al., 2004) and Fuzzy Logic Models (Bennajeh et al., 2018). In addition, adaptive cruise control (ACC) and cooperative adaptive cruise control (CACC) models were developed in the theory-based model group. Unlike the previously mentioned models, which aimed to simulate driver behaviour and identify disturbances in natural traffic, ACC models were designed to eliminate instability from the mechanistic view. Among the ACC and CACC models, the following can be mentioned: linear models (Dias et al., 2015) nonlinear models (Y. Wang et al., 2022) and Model Predictive Control (MPC) (Cheng et al., 2019).

The microscopic models presented in this article use Wiedemann74 (W74) and Wiedemann99 (W99) CFM (Durrani et al., 2016; Wiedemann, 1974; Wiedemann & Reiter, 1992). The W74 and W99 models can be classified as psychophysical models because they are not limited to describing the movement of vehicles (i.e. kinematics). These models encompass more than measurements of vehicle speed, acceleration, and position over time. Instead, Wiedemann's models include psychological and physiological aspects of driver behaviour, such as perception, decisions, and reactions to changes in traffic. Models proposed by Wiedemann take a slightly different approach and are based on drivers' perceptions, as presented in Fig. 1.

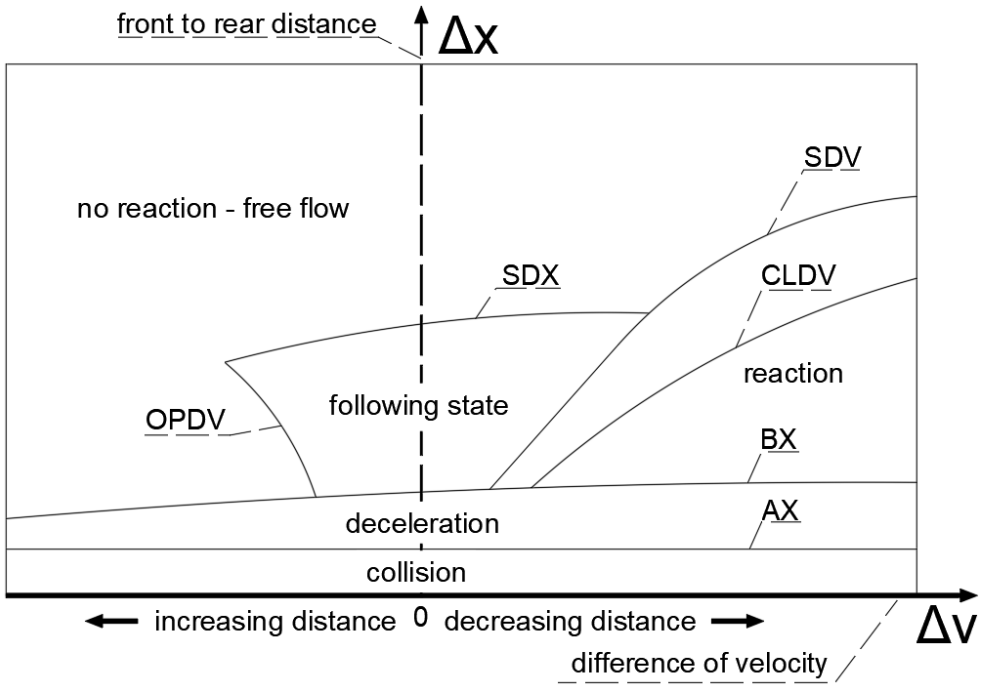

Fig. 1. Wiedemann car-following model based on (PTV Group, 2022) and (Chaudhari et al., 2022)

The main features of the psychophysical model that distinguish it from the kinematic model are the following:

- Perception and driver decisions: the model considers how drivers perceive distances and speeds and how they make decisions about accelerating, braking, and maintaining distance.
- Zones of action: The model divides the driver's reactions into different zones depending on the distance to the preceding vehicle, e.g. free-flowing zone, intended acceleration zone, and comfort braking zone.
- Threshold variables: the model defines different thresholds that initiate specific driver reactions, such as the start of braking or acceleration.

Values present in Fig. 1. can be described as (Chaudhari et al., 2022):

- AX: the desired distance between two vehicles in a stopped condition
- ABX: the desired minimum safe following distance in the moving state, as a lower limit of the following regime
- SDX: the maximum following distance as the upper limit of the following regime
- SDV: the points at long distances (more than SDX) where drivers perceive that they are approaching slower vehicles
- CLDV: points at short distances (less than SDX) where drivers perceive their speeds to be higher than their lead vehicle speeds
- OPDV: the points at short distances (less than SDX) where drivers perceive that they are travelling at a slower speed than the car in front of them.

The Wiedemann 74 model implemented in Vissim software (PTV Group, 2022) is based on the assumption that vehicles maintain a desired distance d. The desired distance is calculated by equation (1):

$$d = Ax + Bx \quad (1)$$

Where:
Ax – "stochastically smeared" base value for standstill distance, Bx – value described by equation (2):

$$Bx = (bx_{add} + bx_{mult} * z) * \sqrt{v} \quad (2)$$

Where:
v – Vehicle speed, z – value from range [0, 1], which is normally distributed around 0.5 with a standard deviation of 0.15, bx_{add}, bx_{mult} – calibration parameters.
The speed of a vehicle n in Wiedemann 74 CFM , (Rakha & Gao, 2010) is described by equation (3):

$$u_n(t + \Delta t) = \min \begin{Bmatrix} 3.6*\left(\frac{s_n(t) - s_j}{BX}\right)^2 \\ 3.6*\left(\frac{s_n(t) - s_j}{BX*EX}\right)^2, u_f \end{Bmatrix} \quad (3)$$

Where:
$u_n(t + \Delta t)$ – the speed of the following vehicle at time $t + \Delta t$ [km/h], $s_n(t)$ – the vehicle spacing between the front bumper of the lead vehicle and front bumper of following vehicle at time t [m], s_j – the vehicle spacing when vehicles are completely stopped in a queue [m], u_f – the space-mean traffic stream free-flow speed [km/h], EX – random variable describing the minimum distance of following vehicles, that can be described by equation (4):

$$EX = EXadd + EXmult * (NRND - RND2_n) \quad (4)$$

Where:
EXadd, EXmult - calibration parameters, NRND – a normally distributed random variable with a default mean value of 0.5 and standard deviation of 0.15, $RND2_n$ - user specified vehicle-specific (where n is the vehicle index) normally distributed random variables with a default mean value of 0.5 and a standard deviation of 0.15.
Wiedemann 99 model (PTV Group, 2022) is more flexible and described by a larger number of parameters, CC0-CC9 that are defined as:

- CC0 - Standstill distance - the distance between the subject vehicle's front and the lead vehicle's rear bumpers.
- CC1 – Driver Sensitivity Factor - gap time distribution (can be calibrated using three macroscopic traffic stream parameters, namely: the expected roadway capacity, traffic density, and free-flow speed)
- CC2 – Following distance oscillation
- CC3 – Threshold for entering 'BrakeBX'
- CC4 – Negative speed difference
- CC5 – Positive speed difference (typically the absolute value of CC4)
- CC6 - Impact of distance on oscillations
- CC7 – Oscillation acceleration
- CC8 – Acceleration from standstill (the maximum acceleration of the vehicle at a speed of 0 km/h) (m/s2)
- CC9 – Maximum acceleration of the vehicle at a speed of 80 km/h (m/s2)

These parameters can be related to the values from Fig. 1. using the following equations (Aghabayk et al., 2013):

$$AX = L + CC0 \quad (5)$$

$$BX = AX + CC1 \times v \quad (6)$$

$$SDX = BX + CC2 \quad (7)$$

$$(SDV)_i = \frac{\Delta x - (SDX)_i}{CC3} - CC4 \quad (8)$$

$$CLDV = \frac{CC6}{17000} \times (\Delta x - L)^2 - CC4 \quad (9)$$

$$OPDV = -\frac{CC6}{17000} \times (\Delta x - L)^2 - \delta . CC5 \quad (10)$$

The speed of a vehicle n in Wiedemann 99 CFM, (Rakha & Gao, 2010) is described by equation (11):

$$u_n(t + \Delta t) = \min \begin{Bmatrix} u_n(t) + 3.6 * \left(CC8 + \frac{CC8 - CC9}{80} u_n(t)\right) \Delta t \\ 3.6 * \frac{s_n(t) - CC0 - L_{n-1}}{u_n(t)}, u_f \end{Bmatrix} \quad (11)$$

Where:
$u_n(t + \Delta t)$ – the speed of the following vehicle at time $t + \Delta t$ [km/h], $u_n(t)$ – the speed of the following vehicle at instant time t [km/h], u_f – the space-mean traffic stream free-flow speed [km/h], $s_n(t)$ – the vehicle spacing between the front bumper of the lead vehicle and front bumper of following vehicle at time t [m], L_{n-1} – the effective length of vehicle *n-1* (the actual length plus a safety margin) [m]
Regardless of which type of CFM is used in a research project, it is crucial to calibrate and validate the models to ensure reliability and an accurate representation of reality. Calibrated traffic models can provide results similar to real-world values (Otković et al., 2020) Often, the calibrated values for certain

parameters may significantly differ from the default values provided by the model author and software provider (E. Hussain et al., 2018). Therefore, it is crucial to monitor the quality of the model and validate it with real-world variables.

2.2. Calculation of vehicle emissions using microscopic models

Instantaneous models are typically based on laws of physics, therefore they are universal and applicable to multiple problems. They are suitable for detailed evaluation of solutions related to intersections, road sections or even subarea networks (Biggs & Akcelik, 1986). A model based on the idea that the instantaneous power of a vehicle needs to overcome the resistive forces is proposed in equation (12) (Leung & Williams, 2000):

$$Z_t = Z_d + Z_r + Z_a + Z_e + Z_m \quad (12)$$

where:
Z_t – instantaneous power equal to the sum of resistances [kW], Z_d – vehicle drive-train resistance [kW], Z_r – tyre rolling resistance [kW], Z_a – aerodynamic drag [kW], Z_e – inertial and gravitational resistance [kW], Z_m – resistance from additional accessories [kW]
Based on the value obtained from equation (12), the fuel consumption value can then be calculated using the following relationship (13) (Leung & Williams, 2000):

$$F_c = \gamma * EC + \beta * Z_t \quad (13)$$

where:
F_c – fuel consumption [ml/min], γ i β – equation coefficients, EC – engine capacity [l], Z_t – total resitances from equation (12).
CO_2 emissions are derived from fuel consumption in a ratio of 2.3kg of CO_2 per 1 l of gasoline, so the model to calculate fuel consumption is also a tool to estimate the carbon dioxide emitted by vehicles.
A different approach that also utilises the dynamics of a vehicle is a calculation of Vehicle Specific Power (VSP), which can be described in general form by equation (14) (Koupal et al., 2005):

$$VSP = (A * v + B * v^2 + C * v^3 + m * v * a)/m \quad (14)$$

where:
VSP – Vehicle Specific Power [kW/metric ton], v – speed [m/s - mps], a – acceleration [m/s^2], m – mass [metric tonnes 1000kg], A – rolling resistance term [kW/mps], B – friction term [kW/mps^2], C – aerodynamic drag term [kW/mps^3]
When values of speed, acceleration and road grade are known, but resistance-related values are unavailable, the VSP model is often utilised by using typical values (United States Environmental Protection Agency, 2002) in equation (15):

$$VSP = v[1.1 + 9.81(a\tan(\sin(grade))) + 0.132] + 0.000302v^3 \quad (15)$$

where:
VSP – Vehicle Specific Power [kW/metric ton],A v – speed [m/s], a – acceleration [m/s^2]
The VSP can then be transformed into the fuel consumption and emissions estimation, similar to the Vehicle Drag approach. While equation (15) is more simplified than 16 due to the fewer components included, it is still useful especially when the data is required to calculate the sum of resistance from eq. (12) is not available. One example is the use of VSP to estimate emissions using sparse trajectory data (Ma et al., 2024).

2.3. Calculation of surrogate safety measures in microsimulation modelling

An accident is an event that occurs unexpectedly and unintentionally. For this reason, it is very challenging to analyse it directly in microscopic traffic simulations. Intentionally modelling an accident does not seem like the right way to approach this problem, as it would make an accident not unexpected at all. One of the solutions to this problem is to use indirect measures, usually called surrogate safety measures (SSM). The stochastic parameters adopted in the simulation models make it possible to define individual preferences and trends in traffic users' behaviour at a reasonable level of approximation. Identifying conflicts and potentially dangerous situations is possible by modelling the relationship between vehicles. These relationships must precede an accident (as presented in Fig. 2.), but they frequently manifest in the absence of an accident. Therefore, by analysing measures that describe different vehicle approximations on the road, the relationship between conflicts

and potential accident risk can be established (Laureshyn & Várhelyi, 2018).

The Surrogate Safety Assessment Model (SSAM) serves as a tool for gathering and conducting initial analyses of SSMs derived from microsimulation models (Gettman et al., 2008). The SSAM is a post-processing tool that utilises vehicle trajectories generated in microsimulation software packages. The usefulness of most algorithms used in microsimulation models for road traffic safety assessment is limited due to their focus on typical driver behaviour and inability to account for vehicle collisions (Xin et al., 2008). Certain simplifications are inevitably necessary, even in the most advanced models. Consequently, the significance of the results as representations of actual road user behaviour may be debatable. Assessing road safety at the microscopic level involves using simulation techniques based on surrogate measures (Oskarbski et al., 2020). The mean traffic volume, median speed, and instantaneous deviations in the values of volume and speed significantly affect the possibility of an incident (Golob et al., 2004). The most common cause of accidents is insufficient headway at high vehicle speeds. (Zou et al., 2023) analysed driver behaviour in highway reconstruction zones and identified components that affect the probability of a conflict. The research results suggest that heightened speed, larger vehicle dimensions, and small radius of curved sections are correlated with an increased likelihood of traffic conflicts arising. Surrogate safety measures include speed, distances between vehicles, traffic-related measures, and lane change manoeuvres (Archer, 2005). Simulation models use measures from traffic conflict theory (Essa & Sayed, 2018). Observing sudden braking and avoidance manoeuvres helps identify traffic conflicts and their connection to real-life accidents (Lord & Washington, 2018). Traffic conflict occurs when two or more road users approach each other, requiring fast and decisive manoeuvres to avoid collision. The method involves observing or simulating the road system and noting conflict situations that could lead to accidents in specific areas.

The use of simulation to estimate changes in traffic safety has also been applied to intersections (M. S. Hussain et al., 2024). Researchers used a current unsignalised intersection to adjust the model. They then simulated a scenario with traffic signals to determine the expected improvement in road traffic safety resulting from reduced conflicts, despite the added delays at red lights.

Several fundamental indicators, indicative of traffic conflicts, have been suggested, e.g., Time To Collision (TTC), Deceleration Rate (DR) and the time interval between collision vehicles, leaving the collision point and arriving at the collision point (Post-Encroachment Time-PET). The most commonly used SSMs of traffic safety in the research was TTC followed by PET and their derivatives (Archer, 2005). These measures are frequently used in traffic safety research to evaluate the importance of potential conflicts and their correlation with accident severity (PIARC, 2004). The aggregated data's effectiveness in calculating the risk of incident occurrence is uncertain (Elvik et al., 2009). However, the ratio of conflicts calculated with surrogate measures to accidents is estimated to be 20,000 to 1 (Gettman et al., 2008). SSMs can replace statistical measures for accidents and their victims. Traffic conflict theory represents a proactive approach to safety research, allowing for analysis and intervention without the necessity of actual accidents occurring.

2.4. Validation of traffic models

One of the important aspects of developing a model is the validation step. Over the years various methodologies customised for conventional traffic modeling issues have been suggested. The typical approach for model validation is the comparison between real distributions and distributions obtained from the model. An example of such a method is Theil's U statistic presented in equation (16) (Aimsun, 2023), given that the calculation is performed for time intervals j

$$U = \frac{\sqrt{\frac{\sum_{j=1}^{m}\left(w_j - v_j\right)^2}{m}}}{\sqrt{\frac{\sum_{j=1}^{m} w_j^2}{m}} + \sqrt{\frac{\sum_{j=1}^{m} v_j^2}{m}}} \tag{16}$$

Where:

w_j – simulated flow at time interval j, v_j – observed flow at time interval j.

When the values are close to 0 there is little or no difference between real and simulated traffic flow values. Values between 0.2 and 0.7 require further investigation, and values greater than 0.7 are unacceptable.

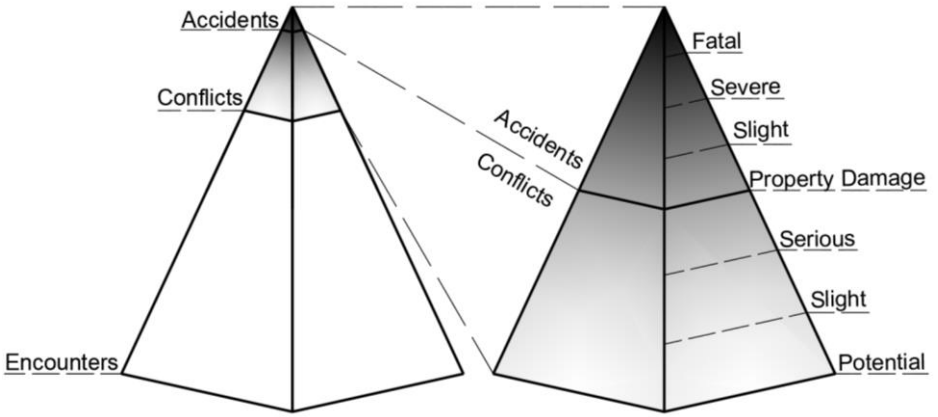

Fig. 2. Pyramid of conflicts based on (Laureshyn & Várhelyi, 2018)

The different metric that is among the most popular for validating traffic flow is the GEH statistic (17) (Aimsun, 2023; Jastrzebski, 2016):

$$\mathrm{GEH} = \sqrt{\frac{2(\mathrm{m}-\mathrm{o})^2}{(\mathrm{m}+\mathrm{o})}} \tag{17}$$

Where:
m – simulated traffic flow, o – observed traffic flow.
While the mathematical form is similar to the chi-squared test it is not a true statistical test (Aimsun, 2023). Depending on the values obtained from the GEH, assumptions can be made:

- Values lower than 5: Good fit
- Values between 5 and 10: Further investigation is required
- Values greater than 10: Unacceptable

Model variables characterising the traffic flow on the road network or its components, such as road sections and intersections (queue lengths, vehicle spacing, delays, number of stops, speed of the traffic flow or individual vehicles, etc.) should also be validated (Oskarbski & Biszko, 2023).

3. Research methodology and model development

It is necessary to gather relevant data to develop a microscopic model. Firstly, the scope of the analysed network needs to be defined. Subsequently, data on the traffic flow volume must be collected. It's crucial to incorporate public transport details when choosing a network to ensure an accurate simulation of real-life traffic conditions. Furthermore, details regarding driver behaviour must be identified for a comprehensive simulation. The data obtained can then be used as input for the model. A more detailed explanation of these steps can be found in sections 3.1 to 3.3.

After completing the model preparation phase, calculations can be performed, and relevant data can be extracted. In this research, metrics were calculated on three primary subjects:

1. Traffic conditions
2. Environmental pollution and energy efficiency
3. Traffic safety

Although the values for traffic conditions can be obtained directly from the VISSIM software, additional external calculations and analyses are required for the metrics related to environmental issues and traffic safety. The process of obtaining these values was described in Sections 3.4 and 3.5.

3.1. Transport network

A test site was chosen to be located on a stretch of provincial road no. 468 ("Morska" street) in Gdynia city. This stretch has a two-by-two-lane cross-section with two lanes in each direction, separated by barriers. The specific location includes three intersections with traffic signals: "Owsiana" Street, "Zbożowa" Street, and "Kcyńska" Street.

The chosen section of the network was replicated in the PTV Vissim microscopic traffic modelling software, with consideration given to actual traffic signal patterns, traffic management, and public

transport (PT) stops. Authentic traffic signal schedules were acquired from the Authority of Roads and Greenery in Gdynia. The developed road network model and the location of bus stops is presented in Fig. 3.

The City of Gdynia has a functioning Intelligent Transport System (ITS) called "TRISTAR". The designated testing features induction loops installed in the pavement near intersection entries and exits. This setup allows for the collection of specific traffic data.

Traffic volume data was collected over three representative weeks in October 2022. Subsequently, this data underwent processing to extrapolate the traffic patterns for each hour on typical days of the week. This methodology enables the identification of peak traffic hours, which served as the focal point for subsequent analysis.

The induction loops enable the capture of the vehicle type, thereby allowing the calculation of the proportion of heavy vehicles on the road. Utilising the PT timetables available on the public transport authority's website the authors of this paper documented the details concerning the number of buses and their respective departure times.

The traffic flow volume, including the share of heavy vehicles and buses, was then inputted into the microscopic model.

3.2. Driver behaviour modelling

Induction loops connected to the TRISTAR system are usually placed so that it is possible to record the speed of vehicles passing through them. The data is recorded for every vehicle separately and can be utilised to create a speed distribution. Modelling speed in microscopic traffic simulation is based on adjusting the desired speed that drivers want to travel. The speed is simulated based on the presence of other vehicles and obstacles on the road. Therefore, to calibrate the model, the speed distribution during free-flow traffic should be extracted from the available data and used as a parameter. After simulation, the actual speed distribution recorded during the peak hour at the intersection should closely match the values calculated in the simulation for the peak hour scenario. The model does not consider the actual distribution of speeds during peak hours, using only the free-flow speed distribution. Data on actual speed is solely used to validate the model, employing data from a separate control group.

Speed data gathered from induction loops near the intersection are distorted due to manoeuvres such as turning, which require drivers to slow down. The authors of this paper decided to use the data from induction loops embedded in pavement near a signalised pedestrian crossing, located on a road section of the same road. This strategy avoids interference from turning manoeuvers, as all vehicles in this road section move forward and stop to let pedestrians pass only during green time. Precise times of beginning and ending, for every traffic signal connected to the Intelligent Transportation System were recorded. The start and end times of the green signal were mapped to the time stamps of the vehicles that passed through the induction loops. Given that upon the start of the green signal, drivers need some time to ramp up their speed, every data recorded up to 30 seconds after the beginning of the green signal was discarded. All data for signals other than green were also discarded because, e.g. during a red signal, a driver may slowly drive through the induction loops while approaching the traffic lights, intending to stop. It was also mentioned that the recorded speed should be related to movement in free-flow traffic, as the presence of other vehicles might influence the actual speed, which will be lower than the desired speed. Since there are two lanes in each direction, it was determined that only values where the total traffic flow volume is considerably low are to be considered. A threshold value of 30 vehicles per 15 minutes was set in every direction. This means that traffic volumes were considered where, on average, there was no more than 1 car per minute in either lane.

Fig. 4. presents the speed values depending on the time elapsed from the beginning of the green signal. Signalised pedestrian crossings change their signal upon manual activation from a pedestrian. Therefore, during nighttime hours, without pedestrians present, there can be a very long green signal for vehicles that lasts several hours. In Fig. 4. the blue colour shows all of the recorded values. The orange colour shows the values filtered under the conditions of undisturbed free-flow traffic. The speed distribution obtained from the selected data is shown in Fig. 5.a. The speed limit on Morska Street is 50 km/h, and only 10% of drivers adhere to it. Another value used in microscopic modelling is the time interval (headway) between vehicles, i.e. the time difference between two appearances on a single point. Unlike speed, this variable should be recorded under traffic conditions with a high

volume of vehicles. This headway represents the "safe space" a driver chooses to maintain following another car. Therefore, the following does not occur in free-flow traffic conditions. For this reason, the distribution of time intervals was extracted for vehicles that passed through induction loops when the traffic flow was at least 400 vehicles in 15 minutes per direction. The results are presented in Fig. 5. b. 90% of the recorded values fall within an interval of up to 5 seconds. It was decided to discard values above 10s, due to the disappearance of the car-following effect at such large intervals.

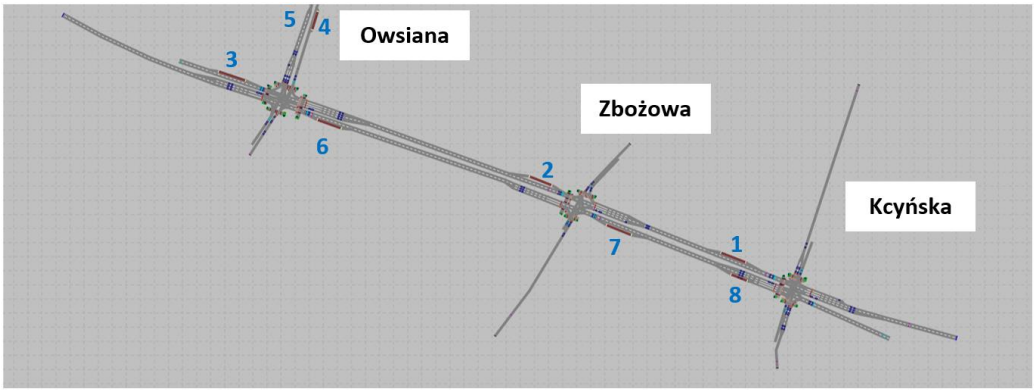

Fig. 3. Network modelled in PTV Vissim software

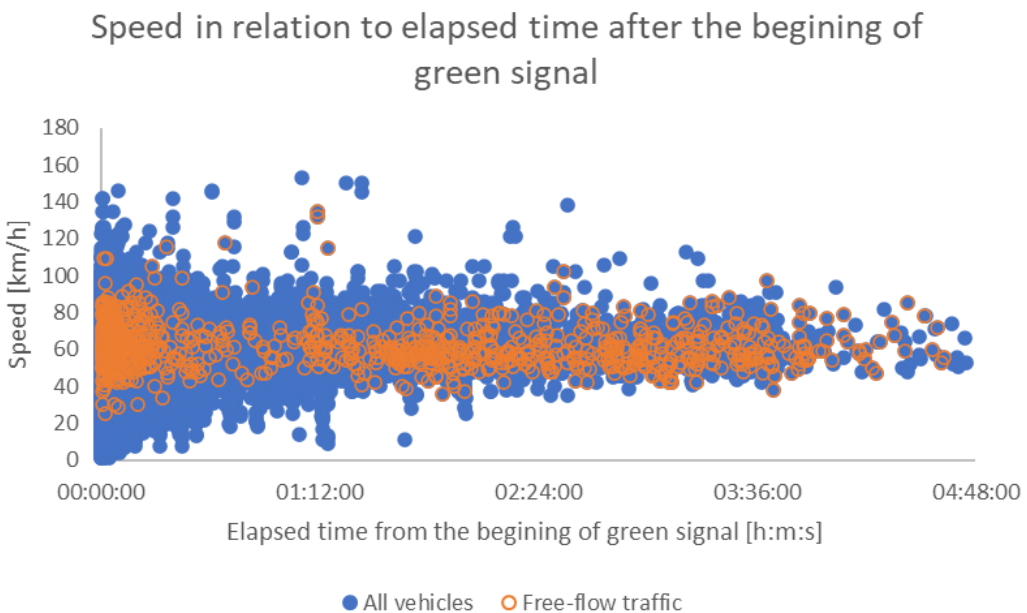

Fig. 4. Vehicle speed concerning the time after the start of the green signal

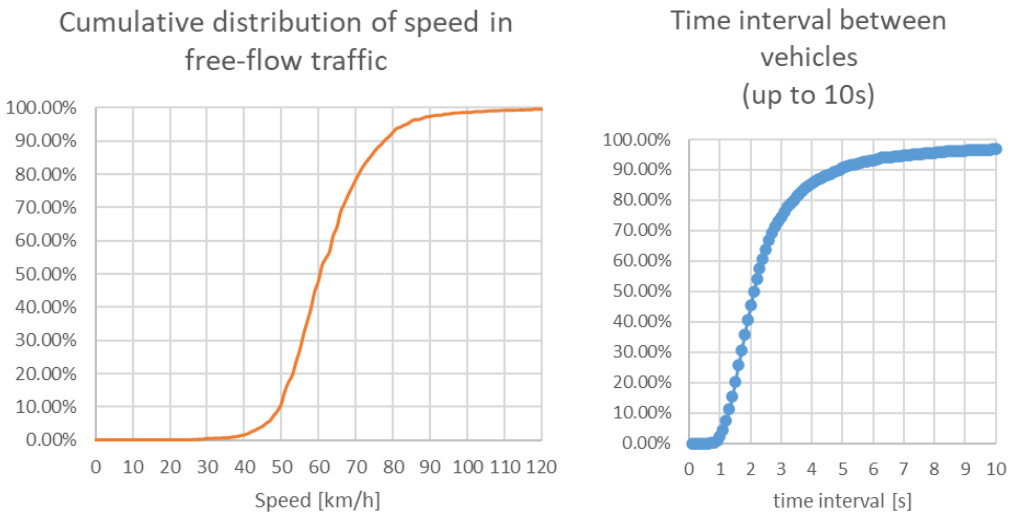

a) b)

Fig. 5. a) Distribution of speed in free-flow traffic, b) Distribution of time intervals between vehicles

3.3. Travel times of public transport vehicles

Public transport operates according to schedule. However, high traffic volumes and congestion also affect buses travelling on roads shared with private vehicles. Due to that, an attempt was made to evaluate the real travel times of city buses that pass through the test site. On-board GPS units for Automatic Vehicle Location (AVL) systems addressed this rather than assuming that PT vehicles adhere perfectly to their schedules.

The scope of the test site allows for the analysis of 6 different segments between pairs of PT stops.

The stops are located differentially to the intersections with traffic lights and the distances between each pair of stops are various. There are numerous methods for calculating travel times between two stops, some of which may include dwell times. These methods assume calculating travel time from the arrival of a PT vehicle at a bus stop to its arrival at the next stop, from departure to departure, from departure to arrival, and from arrival to departure. Two ways of calculating travel times between stops that were included in this study are presented in Fig. 6.:

1) travel time between the departure of a PT vehicle from stop A and its arrival at stop B (smaller values, depicted in blue),
2) travel time between the departure of a PT vehicle from stop A and its departure from stop B (larger values, depicted in orange).

The main purpose of this analysis is to study the impact of traffic conditions on PT travel times, however can also serve as a validation method. The input data for the model consists of timetables, while the model's output provides the time required to travel through the network under current traffic volumes. Therefore analysing GPS data from the PT vehicles aims to determine the average travel time, which is affected by some factors: traffic conditions, the behaviour of bus drivers, traffic control scenarios using traffic signals, etc. Another important aspect is the accuracy of the GPS receivers installed in the vehicles and the method to determine the moment of arrival and departure. An analysis was conducted at six stops to identify potential measurement errors in the TRISTAR system AVL data. This analysis involved comparing manual measurement of actual arrival and departure times with values recorded directly by the system. The measurements were conducted using footage from cameras located at bus stops. Subsequently, average travel times were calculated based on the days from which the average traffic volume values were derived.

3.4. Calculating energy and emissions based on movement resistance

The model described in Section 2.2 was employed for calculating energy consumption and emissions. The equations were implemented in an external module as a code written in the C++ programming

language, following the documentation and templates provided by the software vendor. The module was designed to allow for the use of various equations for different types of vehicles in the microscopic modelling software. This flexibility enables the application of different coefficient values, such as representing varying air resistances for passenger cars and heavy vehicles. In addition, the weight distribution is a parameter that can be introduced directly into the modelling software. The module to calculate emissions pulls the mass value assigned to each vehicle separately.

Given the calculation method, CO2 emissions depend on the vehicle's fuel consumption, and fuel consumption depends on the energy required for the car to move. In addition to the directly calculated values, internal combustion engines continue to operate even when the vehicle is stationary and requires no energy due to the lack of movement. This additional component has been included in the calculations.

3.5. Calculating safety using surrogate safety measures

Surrogate safety measures were examined to assess road traffic safety. To achieve that the trajectories of vehicles were first extracted from the simulation model in a separate file with .trj (as trajectory) format. Then, external software SSAM3 (Surrogate Safety Assessment Method) was used to process the files. The measures that were selected for further analysis are:

1) Total number of conflicts
2) "MaxDeltaV"
3) Time to collision (TTC)

The upper threshold for an encounter to be considered a conflict was set at 1.5 seconds to estimate the level of road traffic safety. Recorded conflicts can then be divided into three main groups based on the angle at which trajectories intersect, as shown in Fig. 7.

Time to collision (TTC) represents the value of time left to a collision between two vehicles if neither vehicle takes any action to avoid it (Hayward, 1972). When analysing conflicts, it is imperative to note that TTC values cannot reach zero seconds. This is because a zero-second TTC would signify a collision, and in a simulated environment, vehicular behaviour is typically structured to mitigate the accident occurrence. Equation (18) can be used to calculate TTC. A minimum assumed TTC value (TTCmin between 0.1 s and 1.5 s) was adopted to define the traffic conflict occurrence.

$$TTC_i = \frac{X_{i-1}(t) - X_i(t) - l_i}{\dot{X}_i(t) - \dot{X}_{i-1}(t)} \quad \forall \dot{X}_i(t) > \dot{X}_{i-1}(t) \tag{18}$$

where:

X -vehicle position, $\dot{X}$ - vehicle speed, i - vehicle following the leader, $i-1$ -lead vehicle, t -moment in time, l -vehicle length.

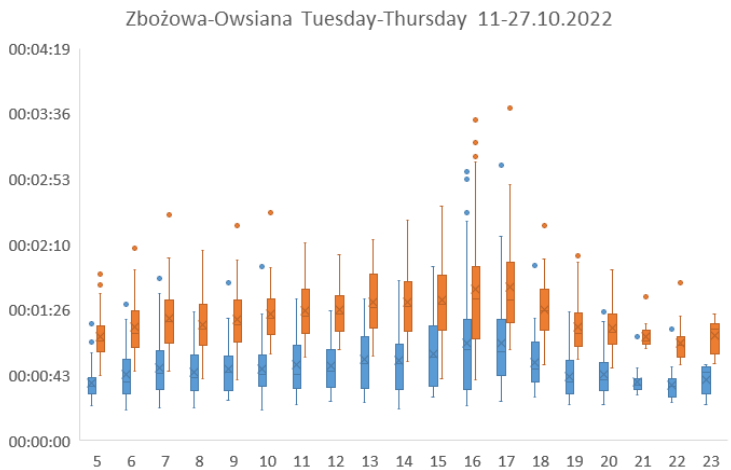

Fig. 6. Average travel times during a typical weekday between two example stops

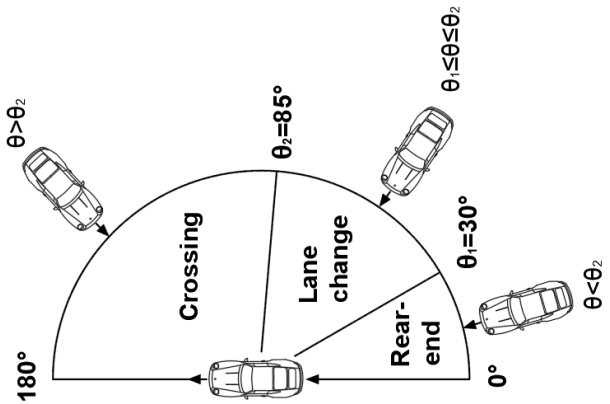

Fig. 7. Conflict types based on (Gettman et al., 2008).

In the event of a conflict, at least one of the vehicles is moving at a certain speed. The maximum speed difference between the vehicles involved in a single conflict is called MaxDeltaV. A larger MaxDeltaV value increases the risk of an accident and its potential severity. The severity of traffic conflict can be determined by comparing the trajectories of two vehicles in terms of direction and speed at the moment of TTCmin occurrence. A conflict is considered severe when the speed difference between vehicles is more than 20 km/h (Yan et al., 2008).

4. Model calibration and validation

The simulation model was developed using the methodology presented in Section 3. The modelling software enables two car-following models to be used: Wiedemann 74 (W74) and Wiedemann 99 (W99). According to the PTV Vissim user guide recommendations (PTV Group, 2022), the models are pre-calibrated to suit the needs of city-oriented behaviour in W74 and motorway-oriented behaviour in W99. Although the test location is in an urban area and the W74 CFM should be suitable, some important specific aspects of the recorded driver behaviour may deviate from the assumptions of this model in Polish traffic conditions. Drivers tend to disobey speed limits. Additionally, the geometry of the urban arterial (two lanes in each direction, physically separated by barriers) can influence driver behaviour.

Free-flow vehicle speed has been adopted for both models based on results presented in Fig. 5a. The W74 model with its initial parameters was decided to be used for the study. To adapt the W99 model to the recorded driver behaviour, the distribution of the headways between vehicles was set according to Fig. 5b. The remaining modifiable parameters were left as default values. Given that the model is based on urban ITS data, there are some limitations on the variables that can be verified due to data availability. This also demonstrates a potential problem for nonresearch projects, where traffic engineers attempt to develop models but lack adequate data. In the calibration process, if the driver behaviour characteristics obtained with the default parameters are not satisfied, the parameters are often changed incrementally with a preset step. The calibration process continues until the modeller is satisfied that convergence between the model and reality has been achieved.

A validation was conducted to verify which car-following models can better represent reality. The variables that were analysed are as follows:

1. Number of vehicles that passed through the modelled network
2. Vehicles speed
3. Public transport travel times

The detailed process of model validation is presented in Sections 4.1-4.3.

4.1. Validation of traffic flow values with GEH

Once the traffic flow values obtained from the test site have been input into the model, verification is required to ensure that the number of vehicles input into the model can pass through the simulation network.

The model output may be lower in traffic volumes than the input data in the case of heavy congestion occurring on the modelled network (while the real-life conditions are better). Data was collected at each intersection exit (3 intersections with a total of 4 exits) to check whether this aspect of the model represents reality. In this case, only vehicles that have successfully reached the intersection exit are counted, not just those that have entered the network.
A GEH metric was used for this validation. Traffic flow values were calculated for the W74 and W99 car-following models at all intersection exits mentioned. The results are presented in Table 1. Satisfactory GEH results were recorded for both models: GEH values below 3 at 11 of the 12 points of the network. In general, coefficient values below 5 are considered correct, and this condition was met completely.
The implication is that, regardless of the CFM model used, there is a convergence between the traffic volumes calculated in the simulation and the values observed at the test site.

4.2. Convergence between vehicle speed distributions

The speed distribution that was an input to the model represents the desired speed. The distribution obtained from the model reflects the speed influenced by traffic conditions. The exits of an intersection located in the middle of the modelled network were chosen as suitable measuring points. The data obtained from the test site and simulations with both CFMs were compared. The findings are illustrated in Fig. 8a. These data represent the speed distribution during a typical peak hour. For an alternative visual representation, the distribution values were standardised and then plotted in Fig. 8b. The x=y line on the graph reflects the observed values. Therefore, the closer the plotted values of the W74 and W99 models are to the x=y line, the more similar the distributions are. In this instance, W99 CFM yields better results, as evident in Fig. 8a. It is significant to note that this similarity arises due to the slower speed of vehicle movement. What's crucial here is that the desired speed distribution input is identical for both CFMs, and the W74 model is intended to be more suitable for urban traffic. However, vehicles in the W74 model travel at higher speeds, resulting in a greater disparity between the simulation and real-world speed distributions.
The distributions calculated from the two CFM models are relatively similar, providing no solid basis for rejecting either model used in the simulations.

4.3. Comparison of public transport travel times

Public transport travel times were calculated in the model using methods presented in Section 3.3. This allows comparison between values obtained through the microscopic simulation and values obtained from GPS. The PT sections included in the model are shown in Table 2. The results of the travel times calculation are presented in Table 3.
Additionally, in Table 2 the comparison between the data from the AVL system and manual measurements are presented, as discussed in Section 3.3. Every section is described by two numbers corresponding to Fig. 3. The presented results show travel time without considering dwell time at a stop (Departure-Arrival - D-A). Travel time includes only the traffic conditions between stops. Due to local conditions during the study, measurements could not be performed for two sections. Mean Average Error (MAE) and Mean Absolute Percentage Error (MAPE) were calculated for the measurements, showing the range of errors relative to the average travel time on the sections. It is evident that on the shortest section between stops, the travel time is characterised by a high MAPE of around 30%. This results from the GPS measurement technique, which is not fully precise, as verified by manual measurements. This is related to errors in vehicle identification at the stop. There are no significant differences in MAE in the remaining sections, but they result in approximately 10% MAPE. Because of these differences, one can expect that in the case of further comparisons with simulation data, there may also be larger differences in average travel times.

Table 1. GEH coefficient for the exits of each intersection

Intersection exit no.	1	2	3	4	5	6	7	8	9	10	11	12
W74	0.84	3.35	1.1	1.07	0.53	1.33	0.96	1.68	0.00	0.28	2.54	2.53
W99	0.39	3.43	1.1	0.72	0.53	1.35	0.84	0.37	0.08	0.28	2.43	0.64

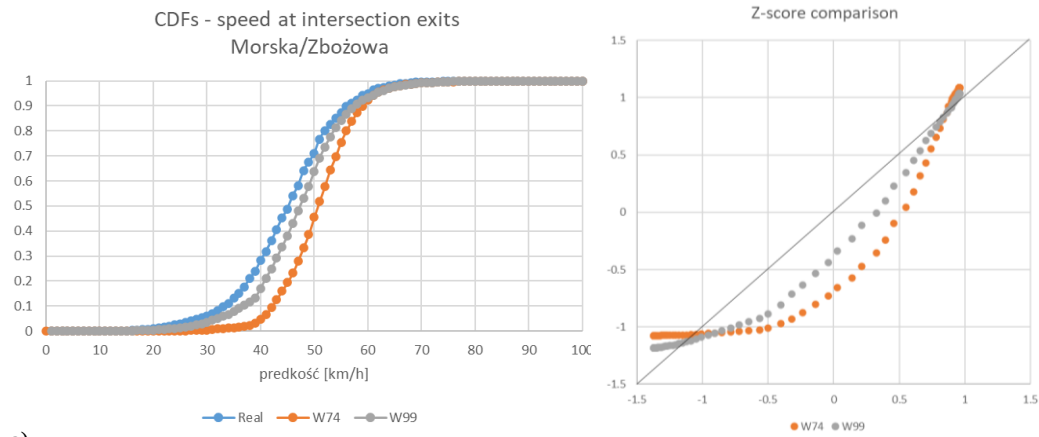

a) b)

Fig. 8. a) speed distributions at the exits of the junction, b) comparison of Z-score values of distributions from the model with measured values

Table 2. PT Sections included in the model

Section	Stops name	Length [m]	Average D-A system [s]	Average D-A measured [s]	TT MAE [s]	TT MAPE [%]
1-2	Kcyńska-Zbożowa	285	30	31	3	11.52
2-3	Zbożowa-Owsiana	444	51	54	3	7.46
2-4	Zbożowa-Jarzębinowa	488	No data			
5-6	Jarzębinowa-Owsiana	210	No data			
6-7	Owsiana-Zbożowa	454	48	45	5	13.29
7-8	Zbożowa-Kcyńska	178	11	12	3	30.01

According to Irish traffic modelling guidelines (Transport Infrastructure Ireland, 2023), the results are considered acceptable if at least 85% of the values obtained from a model have an error of less than 15% or an error of less than 1 minute. In approximately 50% of the evaluated sections, the simulated travel time is around 5% (1% to 7%) compared to the actual measured travel time, accounting for bus stop delays (Departure-Departure - D-D). In particular, travel times demonstrate insignificant variances across the various CF models.

In typical cases, travel times for microsimulations are verified on longer measurement sections to minimise the impact of individual cases with atypical behaviours. However, in this paper, the authors attempted to validate travel times on short sections, which poses a challenge due to the limited sample of PT vehicles. The authors stress the need to refine the methodology for validating the model with PT vehicle travel times to improve the study.

Since the sections between two stops are based on the real locations of the public transport stops from the test site, the length of these sections varies according to the transport network. This means that some distances are very short. For example, the section 7-8 is approximately 180 meters long. Because of this, a difference in travel time of only a few seconds can result in an error larger than 20%. However, this error of just a few seconds in public transport travel time typically indicates high precision in the model's performance.

Considering all the values obtained in Table 3, both the W74 and W99 models perform relatively well. Given that sections of the network are short, it is hard to obtain values with a precision of seconds. There is a randomness component to simulation, so tailoring the values to be exact for one simulation run might

result in discrepancies for different simulation runs. None of the obtained times was longer than 1 minute, and for public transport in the city of Gdynia, the acceptable deviation of bus travel is from -60s up to +180s from the scheduled time. On top of that, in real life bus drivers adjust their travel time dynamically by travelling through some of the road sections faster or slower, in order to arrive at the bus stop closer to the scheduled time. This behavior could not be reproduced in the simulation. To further improve the quality of the results, it might be necessary to distinguish different driving styles in terms of PT or investigate local disturbances, specific to particular stops. These aspects can then be included in the model. On the other hand, if the goal is to consider only typical values, the above findings can be used to exclude certain test site data. This ensures that only representative results are used for validation.

4.4. Validation summary

The main conclusion that can be drawn from Section 4 is that in the validation process, both the W74 and W99 car-following models provided results similar to those measured at the test site. Despite being designed for highway traffic, the W99 model performed slightly better, most likely due to the adaptation of time interval distribution. If we consider typical threshold values to determine convergence, there is no basis to reject either of the applied CFMs for further analysis.

5. Results

The results for the baseline scenario were initially examined during the validation process.

The following scenarios are assessed in this Section:

1. Baseline scenario - validated model (measured traffic volumes and speed distributions, no change in traffic control, permission of Right Turn on Red)
2. Prohibition of Right Turn on Red (RTOR)
3. Traffic flow volume increased by 20%
4. Combined Scenarios 2 and 3: prohibition of RTOR and traffic flow volume increased.

These scenarios are later referenced as Scenario 1, Scenario 2, Scenario 3, and Scenario 4.

Scenario 2 is supposed to represent one possible strategy that can be introduced at signalised intersections. Scenario 3 is intended to represent an increase in the number of vehicles, which may occur temporarily due to additional seasonal traffic in this area, or permanently when considering traffic forecasts for the upcoming years. All scenarios were examined using both W74 and W99 models. The results were collected for a single hour with the highest traffic volume of the day. To better represent real-life conditions, the simulation network was warmed up for one hour before the result data collection, using traffic flow volumes that mirrored those occurring before the peak hour.

The findings in Section 5.1 relate to the traffic conditions derived from the simulation VISSIM software and the external energy and emissions module embedded in the simulation. Section 5.2 outlines the safety-related measures calculated by analysing vehicle trajectories extracted from the simulation using separate SSAM software.

5.1. Results of microscopic modelling

The initial set of analysed findings includes the average delays per vehicle while travelling through the simulated network, the average CO_2 emissions generated idly per vehicle during the time spent in the network (calculated independently of the energy required to overcome resistances), as well as the total CO_2 emissions and overall energy consumption for travelling through the network. The energy value represents the resistances that must be overcome for the vehicles to move (according to the description in Section 2.2). In vehicles with internal combustion engines, energy is generated through fuel consumption For electric vehicles, this energy can be derived from the car battery while accounting for losses, which can be attributed to using lights, air conditioning, and other factors. When vehicles are stationary and do not actively overcome resistances, the value of equation (12) will be zero on multiple occasions. The "idle CO_2" emissions are presented separately to account for this phenomenon.

In total, 8 different models were analysed (scenarios 1-4 for both W74 and W99 models), and the results are presented in Table 4 and Fig. 9.

The prohibition of conditional right turns during red signals and the increased traffic flow volume in scenarios 2, 3, and 4 lead to higher emissions and delays. It was noted that the energy required for vehicles to move is slightly lower in scenarios where no conditional right turns are allowed.

Additionally, using the W99 car-following model resulted in higher values for emissions, energy required, and delays.

Table 3. Average travel times [s] between pairs of stops. A – Arrival, D- Departure

Section	Measured		W74		W99		W74/Measured				W99/Measured			
	D-A	D-D	D-A	D-D	D-A	D-D	D-A		D-D		D-A		D-D	
1-2	36	69	43	63	45	68	+7	19%	-6	-8%	+9	25%	-1	-1%
2-3	62	97	56	77	43	64	-6	-10%	-20	-21%	-19	-31%	-33	-34%
2-4	70	110	59	77	57	77	-12	-16%	-32	-30%	-13	-18%	-33	-30%
5-6	73	113	97	118	99	120	+24	32%	+5	4%	+26	35%	+7	6%
6-7	46	75	57	78	57	78	+11	24%	+3	4%	+11	24%	+3	4%
7-8	13	52	17	39	17	39	+4	28%	-13	-25%	+4	32%	-13	-25%

Since the microscopic simulation only covers a portion of the network during the simulation period, the total energy or emissions value for a complete vehicle travel remains unknown. The results are specific to the modelled area. So in some cases, the total energy value required was lower for scenarios with worse traffic conditions, as in the scenario assuming the prohibition of conditional right-turn. This reduction in energy usage occurred because vehicles no longer engage in constant "stop-and-go" movements during red lights when a queue of cars gradually merges into ongoing traffic. In scenarios 2 and 4, the energy calculated based on equation (12) was slightly lower compared to the corresponding scenarios, as traffic resistances were non-existent when the vehicles remained stationary. However, scenarios where conditional right turns are not allowed experienced higher delays and related idle CO_2 emissions.

When considering relative changes, the values vary among different scenarios and models. This variation primarily occurs because the models are based on different equations, resulting in differing simulated driver behaviour under changing conditions, even when the modifications to the base scenario are consistent. Furthermore, implementing various calibration processes concerning the W74 and W99 parameters in addition to the speed distribution and the distribution of time interval (headway) between vehicles may also impact the results across different scenarios.

Table 4. Idle CO_2 emissions, average delays and total energy required in each scenario and change concerning base scenario 1.

Scenario	Model	Idle CO_2 [g/km]	Avg. delays [s]	Total energy required [kWh]
1	W74	31	47	1220
	W99	35	64	1510
2	W74	33	56	1215
	Change	6.45%	19.15%	-0.41%
	W99	39	78	1501
	Change	11.43%	21.88%	-0.60%
3	W74	36	66	1394
	Change	16.13%	40.43%	14.26%
	W99	39	77	1736
	Change	11.43%	20.31%	14.97%
4	W74	43	92	1411
	Change	38.71%	95.74%	15.66%
	W99	47	104	1694
	Change	34.29%	62.5%	12.19%

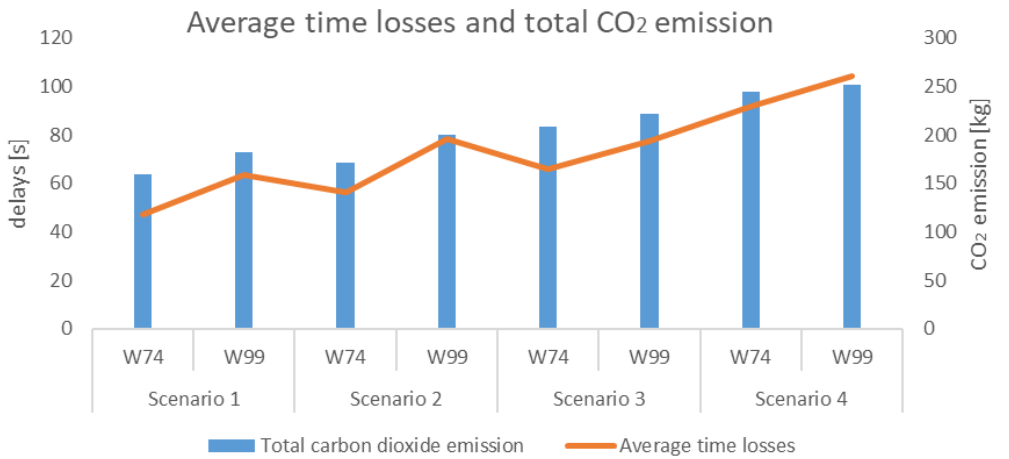

Fig. 9. Total CO_2 emissions and average delays in analysed scenarios

5.2. Results on surrogate safety measures

In different scenarios, different SSM values were calculated. A comparable number of traffic conflicts were observed for the base scenario, with only 3 more for the W74 model. In all other scenarios, there were fewer conflicts when using the W74 model for calculations. Table 5 and Fig. 10. present the total number of traffic conflicts based on the scenario. The prohibition of conditional right-turn signals with base traffic flow volume led to fewer conflicts for W74 and more for W99 than the baseline scenario.

Adding extra traffic flow into the simulation led to a higher frequency of potentially dangerous situations. The increase in the number of conflicts varied for each CFM. Specifically, a 20% increase in traffic volume resulted in a 31% increase in traffic conflicts for W74 and a 52% increase for W99. Removing conditional right turns with increased traffic led to a rise in traffic conflicts, in contrast to scenarios where only the base traffic flow was considered. When comparing scenario 4 to scenario 3, there was a 10% increase in traffic conflicts for W74 and a 16% increase for W99. As for comparing scenario 4 to scenario 2, the number of traffic conflicts increased by 56% for W74 and 53% for W99. When considering the baseline scenario, these differences resulted in a total increase of 45% for W74 and 78% for W99. The conflicts mainly comprised rear-end conflicts (from 382 to 727), with significantly fewer lane-change conflicts (34 to 69) and just a few crossing conflicts.

Table 5. Total number of conflicts for each analysed scenario

Scenario	CFM	crossing	lane change	rear end	total
1	W74	1	34	419	454
	W99	1	49	401	451
2	W74	1	38	382	421
	W99	1	51	466	518
3	W74	1	53	544	598
	W99	1	65	620	686
4	W74	2	48	607	657
	W99	1	69	727	797

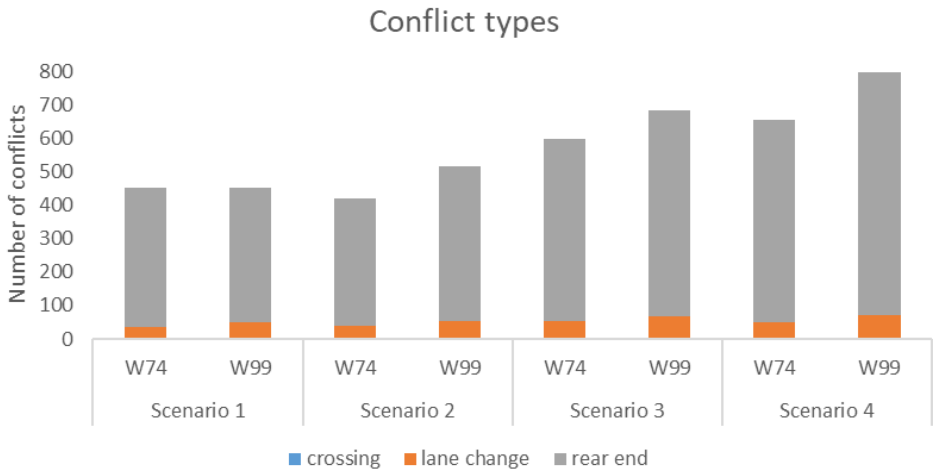

Fig. 10. Total number of conflicts for each scenario

The proportion of traffic conflicts in each class of MaxDeltaV values for the different scenarios is shown in Fig. 11. In general, worse traffic conditions contribute to conflicts at lower speed differences between vehicles. For the scenarios with increased traffic volumes, both the scenarios allowing conditional right turns and the scenarios prohibiting them, despite a higher total number of conflicts, the MaxDeltaV distribution contains more values up to 5 km/h than for the scenarios with baseline traffic volumes. In the case of severe conflicts (difference in speed between vehicles of more than 20 km/h), more traffic conflicts occur in the scenarios with RTOR prohibition as shown in Fig. 12. The lower number of severe traffic conflicts is due to the elimination of the situation where vehicles travelling from the minor entrance meet the traffic stream travelling at higher speeds on the major road. As traffic volume increases, the number of severe conflicts also rises.

The cumulative distributions for each scenario are depicted in Fig. 13. The significant observation is the clear distinction between the distributions at 1.0 s and 1.2 s. This indicates that there were more conflicts with a shorter time to collision in W99 CFM. In essence, utilising the W99 model resulted in more instances where the potential collision was at a closer proximity.

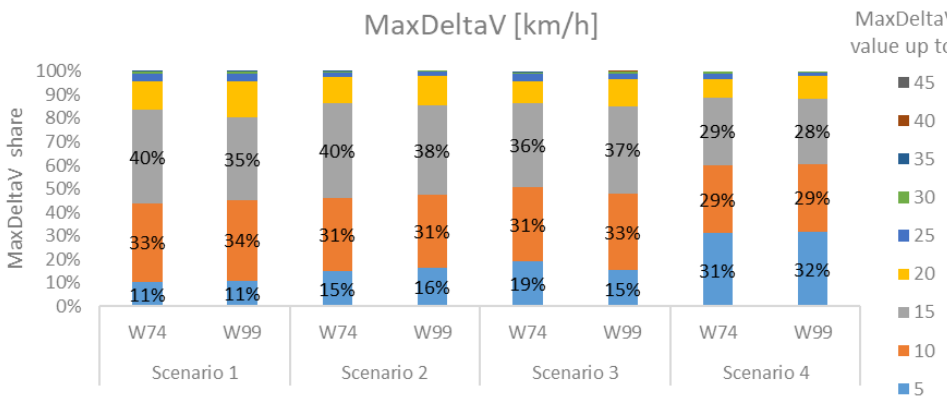

Fig. 11. Distribution of different MaxDeltaV values among scenarios for all conflicts

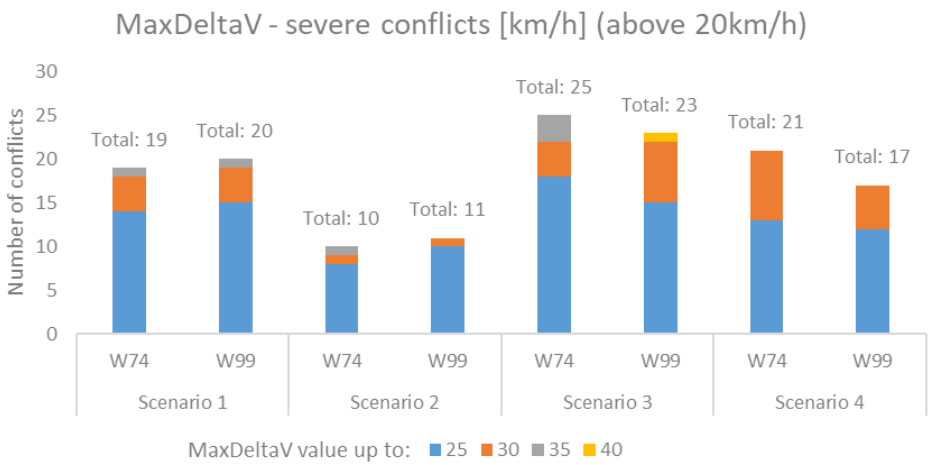

Fig. 12. Distribution of different MaxDeltaV values among analysed scenarios for severe conflicts

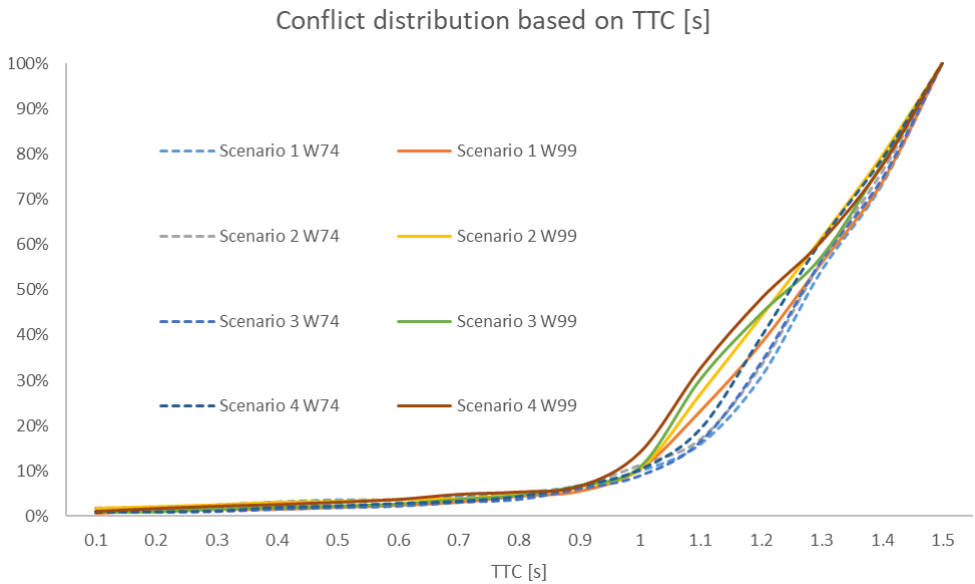

Fig. 13. Distribution of TTC values among analysed scenarios

Table 6 shows a compilation of conflict heatmaps for the analysed scenarios. Regardless of the scenario, it is evident that the largest clusters of traffic conflicts occur in the major approaches at the intersection with Owsiana Street, on the western side of the intersection with Zbożowa Street, and on the eastern side of the intersection with Kcyńska Street. These findings have arisen due to specific local conditions and the formation of clusters of traffic conflicts at the end of the vehicle queue at intersection entrances. During the most congested hour of the day, the afternoon peak, traffic from east to west (passing through intersections with Kcyńska, Zbożowa, and finally Owsiana Street) is predominant. As a result, the traffic signals are strategically set to prioritise the smooth flow of vehicles in this direction. Consequently, there are fewer traffic conflicts on the eastern side of Zbożowa Street as most vehicles move without interruptions from

Kcyńska Street. However, some drivers face challenges to catch the green wave at the intersection with Owsiana Street. On the other hand, traffic flow in the opposite direction (vehicles passing through intersections with Owsiana, Zbożowa, and finally Kcyńska Street) experiences lighter traffic volume, resulting in fewer conflicts on the western side of the intersection with Owsiana Street. This is due to the signal settings, making it impossible for most vehicles to pass through the intersection with Zbożowa Street without stopping. This leads to increased conflicts on the western side of the middle intersection. At the same time, the green signal at the Zbożowa Street intersection allows many vehicles to pass through the intersection with Kcyńska Street without stopping, leading to fewer conflicts on the western side of the intersection with Kcyńska Street.

Comparing the changes between the scenarios shows that:

1) The increase in traffic volume generally contributes to more conflicts, which take place in the same locations as under the baseline scenario
2) The prohibition of RTOR increases the number of conflicts at minor entrances, which are the main beneficiaries of this manoeuvre, especially in a traffic growth scenario (however, the severity of the conflicts is reduced, as shown in Fig. 12)
3) The use of different CFMs contributes to the variable number of conflicts and partly affects the location of the conflicts' clusters, mainly due to differences in the area of the end of vehicle queues and the frequency of their occurrence.

5.3. Discussion

The conducted research revealed that using different car-following models yields varying results, despite similar values being calculated in the validation process and similar traffic volumes and conditions in the baseline scenarios. The results, calculated from simulations highlight the significance of driver behaviour in different car-following models, which can ultimately affect the outcomes. Interestingly, these differences were not identified during the model validation process. In this study, no single car-following model was conclusively determined to be superior to the other. Rather, the differences in results stem from initial decisions made in reproducing driver behaviour, highlighting the need to refine this process. There is an inherent risk that individuals seeking to substantiate a particular stance on safety may selectively utilise models that support their preconceived beliefs. Notably, when changes were implemented to the baseline scenario, both models demonstrated increased delays and CO_2 emissions, with W99 yielding higher values. Regarding traffic safety, the number of conflicts was comparable for both models under existing conditions, but scenarios with additional traffic flow volume simulated using W99 resulted in significantly more conflicts than W74. This situation presents two main challenges:

1) There is currently no reliable method of validation that can confirm with a high degree of certainty that the model accurately represents reality when assessing chosen measures, like traffic conflicts or emissions.
2) There is a practical limit to the amount of data that can be collected and processed to facilitate the development of a detailed simulation.

To address the first issue, thorough research on driver behaviour dynamics and its simulation replication is crucial. For instance, drivers can be classified into different categories based on driving style, and the distribution of each driving category should be determined. In addition, detailed variables such as speed, acceleration/deceleration distribution, car follower behaviour, lane change tendencies, and response to traffic signals need to be established for each category. However, this emphasis on detail highlights the challenge of obtaining such granular data in a general research scenario. When developing microscopic models for regular use, traffic engineers may struggle to collect and process the extensive data needed to meet these requirements for accurate traffic analysis and forecasting.

Comprehensive guidelines should be established to outline specific procedures for data collection, processing, and model validation when developing microscopic simulation models. Establishing standards for these processes would benefit researchers and traffic engineers, leading to more efficient and consistent model development. Although each road scenario may have unique features that require accurate representation, the guidelines should ensure that these features can be effectively incorporated. Uniform guidelines should aim to facilitate consistency and efficiency in microscopic model development, rather than restrict the accurate representation of real-world factors.

Table 6. Conflict heatmaps for analysed scenarios

Scenario:	Wiedemann 74	Wiedemann 99
1	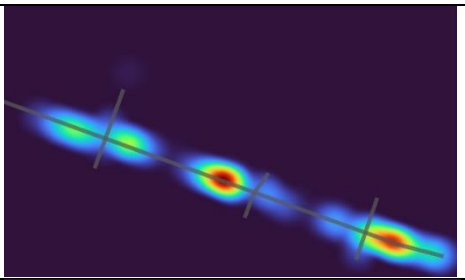	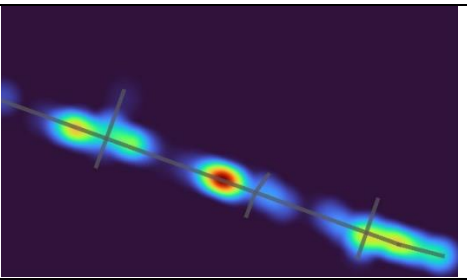
2	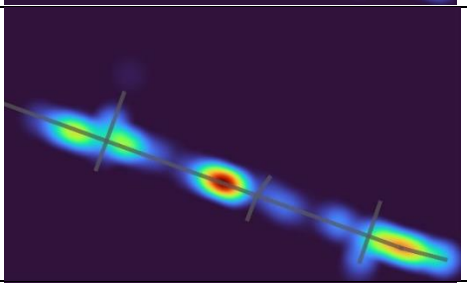	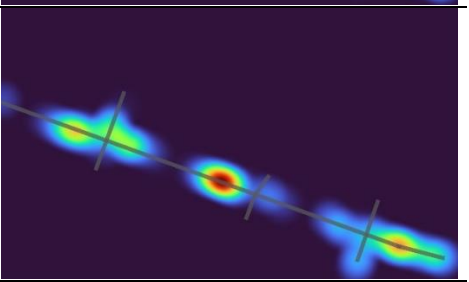
3	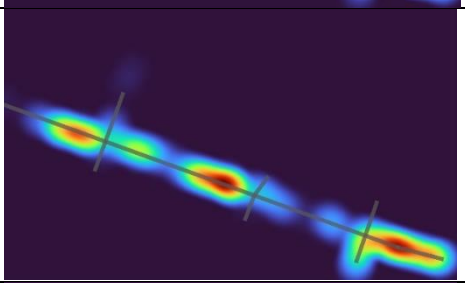	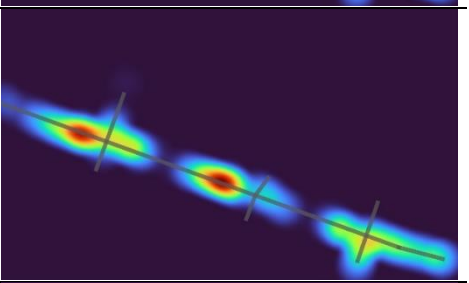
4	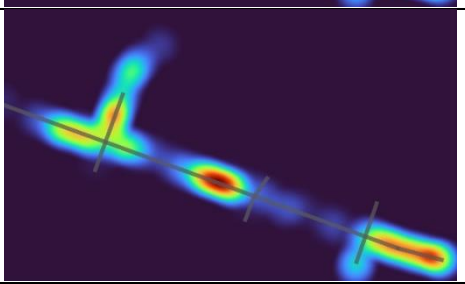	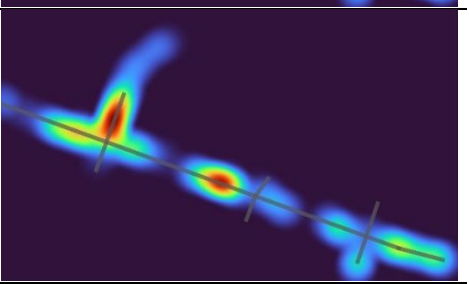

The second crucial aspect of the guidelines should include standard parameters that can be adjusted in models if the person or institution responsible for model development cannot implement the procedures outlined above. Considering the potential significant variations in driver behaviour across different settings, it is advantageous to categorise these parameters into as many subgroups as possible. These may include, but are not limited to, behaviours related to:

1) Location: country, region, rural or urban area (recognising that different cities may exhibit different behaviours)

2) Road infrastructure type: road segments with different numbers of lanes, different types of intersections, and interchanges.

In addition to variations caused by the application of different CFMs, several key observations apply to the obtained results: in better traffic conditions, conflicts at higher speed differences between vehicles arise more frequently; an increase in traffic flow volume leads to a greater number of traffic conflicts; increase in traffic flow volume coupled with the prohibition of RTOR (which leads to deteriorating traffic conditions), results in a higher number of traffic conflicts and a lower proportion of conflicts occurring at higher speed differences. Generally, estimated emissions values exhibit the opposite trend, such that improved traffic conditions lead to lower emission values. Congested roads lead to increased emissions due to frequent stop-and-go movements. However, because vehicles are moving slowly, fewer severe conflicts occur. Although the overall number of traffic conflicts may increase in heavily congested scenarios, the lower speeds at which these conflicts happen mitigate this effect. Slower speeds make it easier to avoid collisions and reduce the likelihood of harm to the involved persons in the event of an incident. In uncongested traffic conditions with fewer vehicles on the road, lower emissions are produced, and theoretically, the total number of conflicts could decrease. With fewer vehicles, interactions between them are expected to occur less frequently. However, when they do occur, the higher speeds at which these encounters happen increase the potential for injury in the event of a car accident.
To achieve the results, microscopic traffic modelling was conducted using the PTV Vissim software. This software enables accurate calculations of vehicle trajectories, allowing for the extraction of values such as acceleration, speed, and location at very short time intervals (0.1 seconds for the models used in this article). This approach enables a comprehensive analysis of conflicts and a fairly accurate estimation of emissions. However, because it requires calculations for every object in the network at each time step, performing these computations using standard methods(not specifically designed for this purpose) would be highly challenging. Furthermore, the computational requirements are notably high, particularly when the simulation involves substantial traffic volumes traversing an extensive road network. Consequently, this necessitates limiting the scope of the microscopic analysis to a selected part of the network. While various software options are available for microscopic traffic modelling, it is important to consider the car-following model used, as these can vary across different software platforms. For this study, the authors utilised the Wiedemann 74 and Wiedemann 99 car-following models, which are implemented by default in PTV Vissim. Conducting conflict analysis directly within Vissim is not feasible. Instead, it is necessary to extract and process vehicle trajectory data using external methods.
Given the computation mentioned above requirements related to the scope of the simulation, when using microscopic traffic modelling, it is important to note that it can only capture a specific network section. It is important to study and critically evaluate various factors thoroughly. For example, the choice to prohibit RTOR leads to lower total energy values but higher average emissions and delays. This occurs because the lower energy values result from unfavourable traffic conditions, where vehicles cannot navigate through the designated section of the network. When vehicles are stuck and unable to move, they can't overcome the resistances used to calculate energy values. Additionally, spending more time in the network causes increased delays and heightened emissions from idling, as the engine continues to run.
The findings underscore the importance of considering specific factors that influence the effectiveness of traffic management. This paper discusses the impact of factors related to traffic control effectiveness, traffic safety, and environmental considerations.

6. Conclusions

This paper investigates the impact of two selected car-following models on the results of microscopic traffic simulations. The authors have proposed techniques to estimate various metrics to evaluate the efficiency of traffic management and control strategies. The study focused on two car-following models: Wiedemann 74 (W74) and Wiedemann 99 (W99). Throughout the validation process, it was determined that both car-following models effectively simulate conditions observed at the test site. However, there were differences in the results related to traffic safety, emissions, and delays. With the W74 model, depending on the scenario, the number of traffic conflicts varied by up to 56%, either increasing or decreasing. On the other hand, with the W99 model, the total conflict count consistently increased

by up to 78%. It is important to note that the different scenarios showed the highest percentage increases for these two car-following models. This highlights the need to explore additional methods for model calibration and validation.

The methodology outlined in the article is designed to help make decisions about mobility planning, control strategies, and traffic arrangement. This is achieved by taking into account estimates related to emissions and traffic safety. More research is needed to improve the effectiveness of the factors that should be considered in these decisions.

Validation of modelled travel times based solely on deviation from the average value seems inadequate due to significant discrepancies in the actual travel times of PT vehicles. In addition, an important element is to verify the measurement data before it is used for modelling at the microscopic level.

In light of the precise nature of microscopic modelling that accurately replicates behaviours, it is imperative to undertake further comprehensive studies to investigate the variables utilised in calibration. The optimal result of these efforts would be the establishment of protocols delineating the methodology and standard values that can be applied in cases where identifying specific behaviours is unfeasible. Comprehensive guidelines are needed to develop microsimulation models, which could include new model validation techniques. This need arises from the observation that both car-following models were considered feasible during the validation stage, yet the results revealed notable disparities.

The authors of this paper intend to further their research by addressing a series of key issues. Their plan includes exploring new methods of collecting data on driver behaviour, focussing on factors such as speed, acceleration, and vehicle distances. They also aim to establish guidelines for validating their models and to develop criteria to support decision-making processes. These criteria would address traffic conditions, emissions and safety, especially regarding traffic conflicts. The ultimate goal is to create a multi-criteria decision analysis framework that can be applied by anyone seeking to utilise microscopic traffic modelling for their specific needs.

The examples of calculations outlined in this paper pertain to various aspects of traffic flow, safety, environmental and climate impacts, and energy efficiency. These serve as a foundation for devising a multi-criteria approach for evaluating the effects of implementing enhancements to the road network and traffic management. This approach should involve an assessment of costs associated with the factors mentioned in the paper and considering infrastructure maintenance concerns. The calculation methods introduced can aid in the planning and oversight of traffic management interventions.

Abbreviations:

PT – Public Transport, CFM – Car-following model, W74/99 – Wiedemann 74/99, SSM – surrogate safety measures, SSAM – surrogate safety assessment method.

References

1. Acuto, F., Coelho, M. C., Fernandes, P., Giuffrè, T., Macioszek, E., & Granà, A. (2022). Assessing the Environmental Performances of Urban Roundabouts Using the VSP Methodology and AIMSUN. *Energies*, *15*(4), 1371. https://doi.org/10.3390/en15041371
2. Aghabayk, K., Sarvi, M., Young, W., & Kautzsch, L. (2013). A novel methodology for evolutionary calibration of vissim by multi-threading. *Australasian Transport Research Forum, ATRF 2013 - Proceedings*, *October*, 1–15. Australian National Audit Office.
3. Ahmed, H. U., Huang, Y., & Lu, P. (2021). A review of car-following models and modeling tools for human and autonomous-ready driving behaviors in micro-simulation. *Smart Cities*, *4*(1), 314–335. https://doi.org/10.3390/smartcities4010019
4. Aimsun (2024). *Aimsun Next 24 User's Manual, Aimsun Next Version 24.0.0*, Barcelona, Spain. Retrieved April 16, 2024, from https://docs.aimsun.com/next/24.0.0/
5. Ajanovic, A., & Haas, R. (2017). The impact of energy policies in scenarios on GHG emission reduction in passenger car mobility in the EU-15. *Renewable and Sustainable Energy Reviews*, *68*, 1088–1096. https://doi.org/10.1016/j.rser.2016.02.013

6. Alonso, A., Monzón, A., & Wang, Y. (2017). Modelling Land Use and Transport Policies to Measure Their Contribution to Urban Challenges: The Case of Madrid. *Sustainability*, *9*(3), 378. https://doi.org/10.3390/su9030378
7. Ambroziak, T., Jachimowski, R., Pyza, D., & Szczepański, E. (2015). Analysis of the Traffic Stream Distribution in Terms of Identification of Areas With the Highest Exhaust Pollution. *Archives of Transport*, *32*(4), 7–16. https://doi.org/10.5604/08669546.1146993
8. Archer, J. (2005). *Indicators for traffic safety assessment and prediction and their application in micro-simulation modelling: A study of urban and suburban intersections.* [Doctoral Dissertation, Royal Institute of Technology]. DiVA portal. https://www.diva-portal.org/smash/get/diva2:7295/FULLTEXT01.pdf
9. Barcelo, J. (Ed.) (2010). *Fundamentals of Traffic Simulation (International Series in Operations Research & Management Science)*. NY, Springer. DOI:10.1007/978-1-4419-6142-6
10. Benjamin, S. C., Johnson, N. F., & Hui, P. M. (1996). Cellular automata models of traffic flow along a highway containing a junction. *Journal of Physics A: Mathematical and General*, *29*(12), 3119. https://doi.org/10.1088/0305-4470/29/12/018
11. Bennajeh, A., Bechikh, S., Said, L. Ben, & Aknine, S. (2018). A fuzzy logic-based anticipation car-following model. In Thanh Nguyen, N., Kowalczyk, R. (Eds.), *Transactions on Computational Collective Intelligence XXX*. *Lecture Notes in Computer Science*, 11120, 200–222. Cham: Springer. https://doi.org/10.1007/978-3-319-99810-7_10
12. Biggs, D. C., & Akcelik, R. (1986). Models for Estimation of Car Fuel Consumption in Urban Traffic. *ITE Journal (Institute of Transportation Engineers)*, *56*(7), 29–32.
13. Bonnafous, A., Gonzalez-Feliu, J., & Routhier, J.-L. (2013). An alternative UGM Paradigm to O-D matrices: the FRETURB model. *13th World Conference on Transport Research (13th WCTR), Rio de Janeiro, Brazil, 15–18 July 2013*. https://shs.hal.science/halshs-00844652v2
14. Cafiso, S., D'Agostino, C., Kieć, M., & Bak, R. (2018). Safety assessment of passing relief lanes using microsimulation-based conflicts analysis. *Accident Analysis and Prevention*, *116*, 94–102. https://doi.org/10.1016/j.aap.2017.07.001
15. Chaudhari, A. A., Srinivasan, K. K., Chilukuri, B. R., Treiber, M., & Okhrin, O. (2022). Calibrating Wiedemann-99 Model Parameters to Trajectory Data of Mixed Vehicular Traffic. In *Transportation Research Record: Journal of the Transportation Research Board*, *2676*(1), 718–735. https://doi.org/10.1177/03611981211037543
16. Cheng, S., Li, L., Mei, M. M., Nie, Y. L., & Zhao, L. (2019). Multiple-Objective Adaptive Cruise Control System Integrated with DYC. *IEEE Transactions on Vehicular Technology*, *68*(5), 4550–4559. https://doi.org/10.1109/TVT.2019.2905858
17. Creutzig, F., Roy, J., Lamb, W. F., Azevedo, I. M. L., Bruine De Bruin, W., Dalkmann, H., Edelenbosch, O. Y., Geels, F. W., Grubler, A., Hepburn, C., Hertwich, E. G., Khosla, R., Mattauch, L., Minx, J. C., Ramakrishnan, A., Rao, N. D., Steinberger, J. K., Tavoni, M., Ürge-Vorsatz, D., & Weber, E. U. (2018). Towards demand-side solutions for mitigating climate change. *Nature Climate Change*, *8*(4), 268–271. https://doi.org/10.1038/s41558-018-0121-1
18. Dias, J. E. A., Pereira, G. A. S., & Palhares, R. M. (2015). Longitudinal Model Identification and Velocity Control of an Autonomous Car. *IEEE Transactions on Intelligent Transportation Systems*, *16*(2), 776–786. https://doi.org/10.1109/TITS.2014.2341491
19. Durrani, U., Lee, C., & Maoh, H. (2016). Calibrating the Wiedemann's vehicle-following model using mixed vehicle-pair interactions. *Transportation Research Part C: Emerging Technologies*, *67*, 227–242. https://doi.org/10.1016/j.trc.2016.02.012
20. EEA (2024). *Greenhouse gas emissions by source sector*. [Data set]. European Environment Agency. https://doi.org/10.2908/ENV_AIR_GGE
21. Elvik, R., Hoye, A., Vaa, T., & Sorensen, M. (2009). Part II Road Safety Measures. In Elvik, R., Høye, A., Vaa, T. & Sørensen, M. (Eds.), *The Handbook of Road Safety Measures* (2nd ed, 144-1092). Emerald Group Publishing. https://doi.org/10.1108/9781848552517

22. Essa, M., & Sayed, T. (2018). Traffic conflict models to evaluate the safety of signalized intersections at the cycle level. *Transportation Research Part C: Emerging Technologies*, *89*, 289–302. https://doi.org/10.1016/j.trc.2018.02.014
23. Gavanas, N., Pozoukidou, G., & Verani, E. (2016). Integration of LUTI models into sustainable urban mobility plans (SUMPs). *European Journal of Environmental Sciences*, *6*(1), 11–17. https://doi.org/10.14712/23361964.2016.3
24. Gazis, D. C., Herman, R., & Rothery, R. W. (1961). Nonlinear Follow-the-Leader Models of Traffic Flow. *Operations Research*, *9*(4), 545–567. https://doi.org/10.1287/opre.9.4.545
25. Gerlough, D. L., & Huber, M. J. (1975). *Traffic Flow Theory. A Monograph.* (TRB Special Report 165). National Research Council. http://onlinepubs.trb.org/Onlinepubs/sr/sr165/165.pdf
26. Gettman, D., Sayed, T., Pu, L., & Shelby, S. (2008*). Surrogate Safety Assessment Model and Validation: Final Report.* (Report No. Fhwa-Hrt-08-51). U.S. Department of Transportation, Federal Highway Administration. https://www.fhwa.dot.gov/publications/research/safety/08051/08051.pdf
27. Gipps, P. G. (1981). A Behavioral car-following model for Computer simulation. *Transportation Research Part B: Methodological*, *15*(2), 105–111. https://doi.org/https://doi.org/10.1016/0191-2615(81)90037-0
28. Givoni, M., Beyazit, E., & Shiftan, Y. (2016). The use of state-of-the-art transport models by policy-makers – Beauty in simplicity? *Planning Theory & Practice*, *17*(3), 385–404. https://doi.org/10.1080/14649357.2016.1188975
29. Golob, T. F., Recker, W. W., & Alvarez, V. M. (2004). Freeway safety as a function of traffic flow. *Accident Analysis & Prevention*, *36*(6), 933–946. https://doi.org/10.1016/j.aap.2003.09.006
30. Gore, N., Chauhan, R., Easa, S., & Arkatkar, S. (2023). Traffic Conflict Assessment Using Macroscopic Traffic Flow Variables: A Novel Framework for Real-Time Applications. *Accident Analysis & Prevention*, *185*, 107020. https://doi.org/10.1016/j.aap.2023.107020
31. Han, J., Wang, X., & Wang, G. (2022). Modeling the Car-Following Behavior with Consideration of Driver, Vehicle, and Environment Factors: A Historical Review. *Sustainability*, *14*(13), 8179. https://doi.org/10.3390/su14138179
32. Hayward, J. C. (1972). Near-miss determination through use of a scale of danger. *Highway Research Record*, *384*, 22–34. http://onlinepubs.trb.org/Onlinepubs/hrr/1972/384/384-004.pdf
33. Hussain, E., Ahmed, S. I., & Ali, M. S. (2018). Modeling the effects of rainfall on vehicular traffic. *Journal of Modern Transportation*, *26*(2), 133–146. https://doi.org/10.1007/s40534-018-0155-0
34. Hussain, M. S., Bahrha, G., & Goswami, A. K. (2024). An integrated VISSIM-SSAM approach to predicting and mitigating pedestrian crashes and severity along urban crossings. *Case Studies on Transport Policy*, *15*, 101153. https://doi.org/10.1016/j.cstp.2024.101153
35. Jacyna, M., Wasiak, M., Kłodawski, M., & Gołębiowski, P. (2017). Modelling of Bicycle Traffic in the Cities Using VISUM. *Procedia Engineering*, *187*, 435–441. https://doi.org/10.1016/j.proeng.2017.04.397
36. Jacyna, M., Zochowska, R., Sobota, A., & Wasiak, M. (2021). Scenario analyses of exhaust emissions reduction through the introduction of electric vehicles into the city. *Energies*, *14*(7), 2030. https://doi.org/10.3390/en14072030
37. Jacyna, M., Zochowska, R., Sobota, A., & Wasiak, M. (2022). Decision support for choosing a scenario for organizing urban transport system with share of electric vehicles. *Scientific Journal of Silesian University of Technology. Series Transport*, *117*, 69–89. https://doi.org/10.20858/sjsutst.2022.117.5
38. Jamroz, K., Budzynski, M., Romanowska, A., Zukowska, J., Oskarbski, J., & Kustra, W. (2019). Experiences and Challenges in Fatality Reduction on Polish Roads. *Sustainability*, *11*(4), 959. https://doi.org/10.3390/su11040959
39. Jastrzebski, W. (2016). Blaski i cienie statystyki GEH do oceny poprawności modeli ruchu. *Transport Miejski i Regionalny*, *6*, 24–26. https://yadda.icm.edu.pl/baztech/element/bwmeta1.element.baztech-8786afa3-1ab2-4843-ab2c-52409c928a66/c/TMiR_6_2016_Jastrzebski.pdf

40. Jayakrisham, R., Mahmassani, H. S., & Yu, T. Y. (1994). An evaluation tool for advanced traffic information and management systems in urban networks. *Transportation Research Part C: Emerging Technologies*, *2*(3), 129–147. https://doi.org/10.1016/0968-090X(94)90005-1
41. Koupal, J., Landman, L., Nam, E., Warila, J., Scarbro, C., Glover, E., & Giannelli, R. (2005). *MOVES2004 Energy and Emission Inputs*. *Draft Report* (Report No. EPA420-P-05-003). United States Environmental Protection Agency. https://nepis.epa.gov/Exe/ZyPDF.cgi/P1001DAQ.PDF?Dockey=P1001DAQ.PDF
42. Kristoffersson, I. (2013). Impacts of time-varying cordon pricing: Validation and application of mesoscopic model for Stockholm. *Transport Policy*, *28*, 51–60. https://doi.org/10.1016/j.tranpol.2011.06.006
43. Laureshyn, A., & Várhelyi, A. (2018). *The Swedish Traffic Conflict Technique: observer's manual*. Lund University.
44. Law, T. H., Noland, R. B., & Evans, A. W. (2011). The sources of the Kuznets relationship between road fatalities and economic growth. *Journal of Transport Geography*, *19*(2), 355–365. https://doi.org/10.1016/j.jtrangeo.2010.02.004
45. Leung, D. Y. C., & Williams, D. J. (2000). Modelling of motor vehicle fuel consumption and emissions using a power-based model. *Environmental Monitoring and Assessment*, *65*(1–2), 21–29. https://doi.org/10.1007/978-94-010-0932-4_3
46. Liu, H., Xiong, Z., & Gayah, V. V. (2024). Quantifying the Impacts of Right-Turn-on-Red, Exclusive Turn Lanes and Pedestrian Movements on the Efficiency of Urban Transportation Networks. *International Journal of Transportation Science and Technology*. https://doi.org/10.1016/j.ijtst.2024.02.007
47. Lord, D., & Washington, S. (2018). *Safe Mobility: Challenges, Methodology and Solutions. Transport and Sustainability, 11*. Emerald Publishing. https://doi.org/10.1108/S2044-9941201811
48. Ma, W., Liu, Y., Kofi Alimo, P., & Wang, L. (2024). Vehicle Carbon Emission Estimation for Urban Traffic based on Sparse Trajectory Data. *International Journal of Transportation Science and Technology*. https://doi.org/10.1016/j.ijtst.2024.01.010
49. Masson-Delmotte, V., Zhai, P., Pörtner, H.-O., Roberts, D., Skea, J., Shukla, P. R., & Pirani, A. (2018). *Special Report: Global warming of 1.5°C.* IPCC. https://www.ipcc.ch/sr15/
50. May, A. D. (1990). *Traffic flow fundamentals*. Englewood Cliffs, NJ: Prentice-Hall.
51. Meng, D., Song, G., Wu, Y., Zhai, Z., Yu, L., & Zhang, J. (2021). Modification of Newell's car-following model incorporating multidimensional stochastic parameters for emission estimation. *Transportation Research Part D: Transport and Environment*, *91*, 102692. https://doi.org/10.1016/j.trd.2020.102692
52. Newell, G. F. (2002). A simplified car-following theory: a lower order model. *Transportation Research Part B: Methodological*, *36*(3), 195–205. https://doi.org/10.1016/S0191-2615(00)00044-8
53. Ortuzar, J. de D., Willumsen, L. G., Ortúzar, J. D. D., & Willumsen, L. G. (2011). *Modelling Transport (4th ed.)*. John Wiley & Sons. https://doi.org/10.1002/9781119993308
54. Oskarbski, J., Birr, K., & Żarski, K. (2021). Bicycle traffic model for sustainable urban mobility planning. *Energies*, *14*(18), 5970. https://doi.org/10.3390/en14185970
55. Oskarbski, J., & Biszko, K. (2023). Estimation of Vehicle Energy Consumption at Intersections Using Microscopic Traffic Models. *Energies*, *16*(1), 233. https://doi.org/10.3390/en16010233
56. Oskarbski, J., Kamiński, T., Kyamakya, K., Chedjou, J. C., Żarski, K., & Pędzierska, M. (2020). Assessment of the speed management impact on road traffic safety on the sections of motorways and expressways using simulation methods. *Sensors*, *20*(18), 5057. https://doi.org/10.3390/s20185057
57. Otković, I. I., Deluka-Tibljaš, A., & Šurdonja, S. (2020). Validation of the calibration methodology of the micro-simulation traffic model. *Transportation Research Procedia*, *45*, 684–691. https://doi.org/10.1016/j.trpro.2020.02.110
58. PIARC (2004). *Road Safety Manual*. World Road Association PIARC, Paris.
59. PTV Group (2022). *PTV Vissim 2022 User Manual*. PTV Planung Transport Verkehr GmbH, Haid-und-Neu-Str. 1, 76131 Karlsruhe, Germany.

60. Rakha, H., & Gao, Y. (2010). *Calibration of steady-state car-following models using macroscopic loop detector data*. *Final Report* (Report No. VT-2008-01, 24). Virginia Tech Transportation Institute. https://www.mautc.psu.edu/docs/VT-2008-01.pdf
61. Ritchie, H., Roser, M., & Rosado, P. (2024*). Energy Production and Consumption*. Our World In Data. First published in July 2020 and last revised in January 2024. Retrieved November 7 from https://ourworldindata.org/energy-production-consumption
62. Roselló, X., Langeland, A., & Viti, F. (2016). Public Transport in the Era of ITS: The Role of Public Transport in Sustainable Cities and Regions. In Gentile, G., Noekel, K. (Eds.), Modelling Public Transport Passenger Flows in the Era of Intelligent Transport Systems. Springer Tracts on Transportation and Traffic, 3-27. Cham: Springer. https://doi.org/10.1007/978-3-319-25082-3_4
63. Shah, D., Lee, C., & Kim, Y. H. (2023). Modified Gipps model: a collision-free car following model. *Journal of Intelligent Transportation Systems*, 1–14. https://doi.org/10.1080/15472450.2023.2289149
64. Shang, M., Rosenblad, B., & Stern, R. (2022). A novel asymmetric car following model for driver-assist enabled vehicle dynamics. *IEEE Transactions on Intelligent Transportation Systems*, *23*(9), 15696–15706. https://doi.org/10.1109/TITS.2022.3145292
65. Si, Z., Hossain, M. A., & Tanimoto, J. (2023). An improved microscopic traffic model for heterogeneous vehicles using the vehicle's mass effect. *Heliyon*, *9*(6), e16731. https://doi.org/10.1016/j.heliyon.2023.e16731
66. Sider, T. M. N., Alam, A., Farrell, W., Hatzopoulou, M., & Eluru, N. (2014). Evaluating vehicular emissions with an integrated mesoscopic and microscopic traffic simulation. *Canadian Journal of Civil Engineering*, *41*(10), 856–868. https://doi.org/10.1139/cjce-2013-0536
67. Sims, R., Schaeffer, R., Creutzig, F., Cruz-Núñez, X., D'Agosto, M., Dimitriu, D., Meza, M. J. F., Fulton, L., Kobayashi, S. O. L., McKinnon, A., Newman, P., Ouyang, M., Schauer, J. J., Sperling, D., & Tiwari, G. (2014). Chapter 8: Transport. In Edenhofer,O., Pichs-Madruga, R., Sokona, Y., Farahani, E., Kadner, S., Seyboth, K., Adler, A., Baum, I., Brunner, S., Eickemeier, P., Kriemann, B., Savolainen, J., Schlömer, S., von Stechow, C., Zwickel, T., & Minx, J. C. (Eds.), *Climate Change 2014: Mitigation of Climate Change. Contribution of Working Group III to the Fifth Assessment Report of the Intergovernmental Panel on Climate Change*, 599–670. Cambridge University Press, Cambridge, United Kingdom and New York, NY, USA.
68. Singh, R., & Dowling, R. (1999). Improved speed-flow relationships: Application to transportation planning models. In Donnely, R. (Ed.), *Proceedings of the Seventh TRB Conference on the Application of Transportation Planning Methods*, 340–349. TRB. https://onlinepubs.trb.org/onlinepubs/trispdfs/00939750.pdf
69. Sivakumar, A. (2007). *Modelling transport: A Synthesis of Transport Modelling Methodologies*. Lonon, UK: Imperial College London.
70. Small, M., Jordan, P., Anyala, M., Shelton, D., & Stapleton, R. (2023). Assessing The Maturity Of National Road Safety Management Systems. *ADB Sustainable Development Working Paper Series* (Paper No. 85). https://dx.doi.org/10.22617/WPS230159-2
71. Smit, R., Smokers, R., & Rabe, E. (2007). A new modelling approach for road traffic emissions: VERSIT+. *Transportation Research Part D: Transport and Environment*, *12*(6), 414–422. http://dx.doi.org/10.1016/j.trd.2007.05.001
72. Szarata, A., Ostaszewski, P., & Mirzahossein, H. (2023). Simulating the impact of autonomous vehicles (AVs) on intersections traffic conditions using TRANSYT and PTV Vissim. *Innovative Infrastructure Solutions*, *8*(6), 164. https://doi.org/10.1007/s41062-023-01132-7
73. Tak, S., Kim, S., Lee, D., & Yeo, H. (2018). A comparison analysis of surrogate safety measures with car-following perspectives for advanced driver assistance system. *Journal of Advanced Transportation*, *2018*. https://doi.org/10.1155/2018/8040815
74. Transport Infrastructure Ireland. (2023). *Project Appraisal Guidelines Unit 5.1 – Construction of Transport Models* (Publication No. PE-PAG-02015). https://www.tiipublications.ie/library/PE-PAG-02015-02.pdf

75. United Nations. (2015). *Transforming Our World: The 2030 Agenda for Sustainable Development. Resolution Adopted by the General Assembly on 25 September 2015*. (Resolution No. A/RES/70/1). General Assembly of the United Nations. https://documents.un.org/doc/undoc/gen/n15/291/89/pdf/n1529189.pdf
76. United States Environmental Protection Agency (2002). *Methodology for Developing Modal Emission Rates for EPA's Multi-Scale Motor Vehicle and Equipment Emission System* (Report. No. EPA420-P-02-027). United States EPA. https://nepis.epa.gov/Exe/ZyPDF.cgi/P10022SD.PDF?Dockey=P10022SD.PDF
77. Wang, L., Abdel-Aty, M., Wang, X., & Yu, R. (2018). Analysis and comparison of safety models using average daily, average hourly, and microscopic traffic. *Accident Analysis and Prevention*, *111*, 271–279. https://doi.org/10.1016/j.aap.2017.12.007
78. Wang, W. H., Zhang, W., Li, D. H., Hirahara, K., & Ikeuchi, K. (2004). Improved action point model in Traffic flow based on driver's cognitive mechanism. *2004 IEEE Intelligent Vehicles Symposium; Parma, Italy, June 14-17*, 447–452. https://doi.org/10.1109/ivs.2004.1336425
79. Wang, Y., Wang, Z., Han, K., Tiwari, P., & Work, D. B. (2022). Gaussian Process-Based Personalized Adaptive Cruise Control. *IEEE Transactions on Intelligent Transportation Systems*, *23*(11), 21178–21189. https://doi.org/10.1109/TITS.2022.3174042
80. Wefering, F., Rupprecht, S., Bührmann, S., Böhler-Baedeker, S., Granberg, M., Vilkuna, J., Saarinen, S., Backhaus, W., Laubenheimer, M., Lindenau, M., Vanegmond, P., & Wegeler, G. (2014). *Guidelines for developing and Implementing a Sustainable Urban Mobility Plan*. European Commission.
81. Wiedemann, R. (1974). *Simulation des Strassenverkehrsflusses* (in German). Schtiftenreibe des Institus fur Verkehrswesen der Universitat Karlsruhe.
82. Wiedemann, R., & Reiter, U. (1992). Microscopic traffic simulation: the simulation system MISSION, background and actual state. In Brackstone, M.A., & McDonald, M., *CEC project ICARUS (V1052) Final report* (2, appendix A). Brussels: CEC.
83. Xin, W., Hourdos, J., & Michalopoulos, P. (2008). *Enhanced Micro-Simulation Models for Accurate Safety Assessment of Traffic Management ITS Solutions. Final Report* (Report No. CTS 08-17). Department of Civil Engineering, University of Minnesota. https://cts-d8resmod-prd.oit.umn.edu/pdf/cts-08-17.pdf
84. Yan, X., Abdel-Aty, M., Radwan, E., Wang, X., & Chilakapati, P. (2008). Validating a driving simulator using surrogate safety measures. *Accident Analysis and Prevention*, *40*(1), 274–288. https://doi.org/10.1016/j.aap.2007.06.007
85. Zhang, T. T., Jin, P. J., McQuade, S. T., Bayen, A., & Piccoli, B. (2024). Car-Following Models: A Multidisciplinary Review. *ArXivLabs*, *ArXiv:2304.07143v4*. http://arxiv.org/abs/2304.07143
86. Zhou, Z., Li, L., Qu, X., & Ran, B. (2024). A self-adaptive IDM car-following strategy considering asymptotic stability and damping characteristics. *Physica A: Statistical Mechanics and Its Applications*, *637*, 129539. https://doi.org/10.1016/j.physa.2024.129539
87. Zou, H., Zhu, S., Jiang, R., Chen, Q., Wu, J., Wang, P., & Diao, C. (2023). Traffic conflicts in the lane-switching sections at highway reconstruction zones. *Journal of Safety Research*, *84*, 280–289. https://doi.org/10.1016/j.jsr.2022.11.004